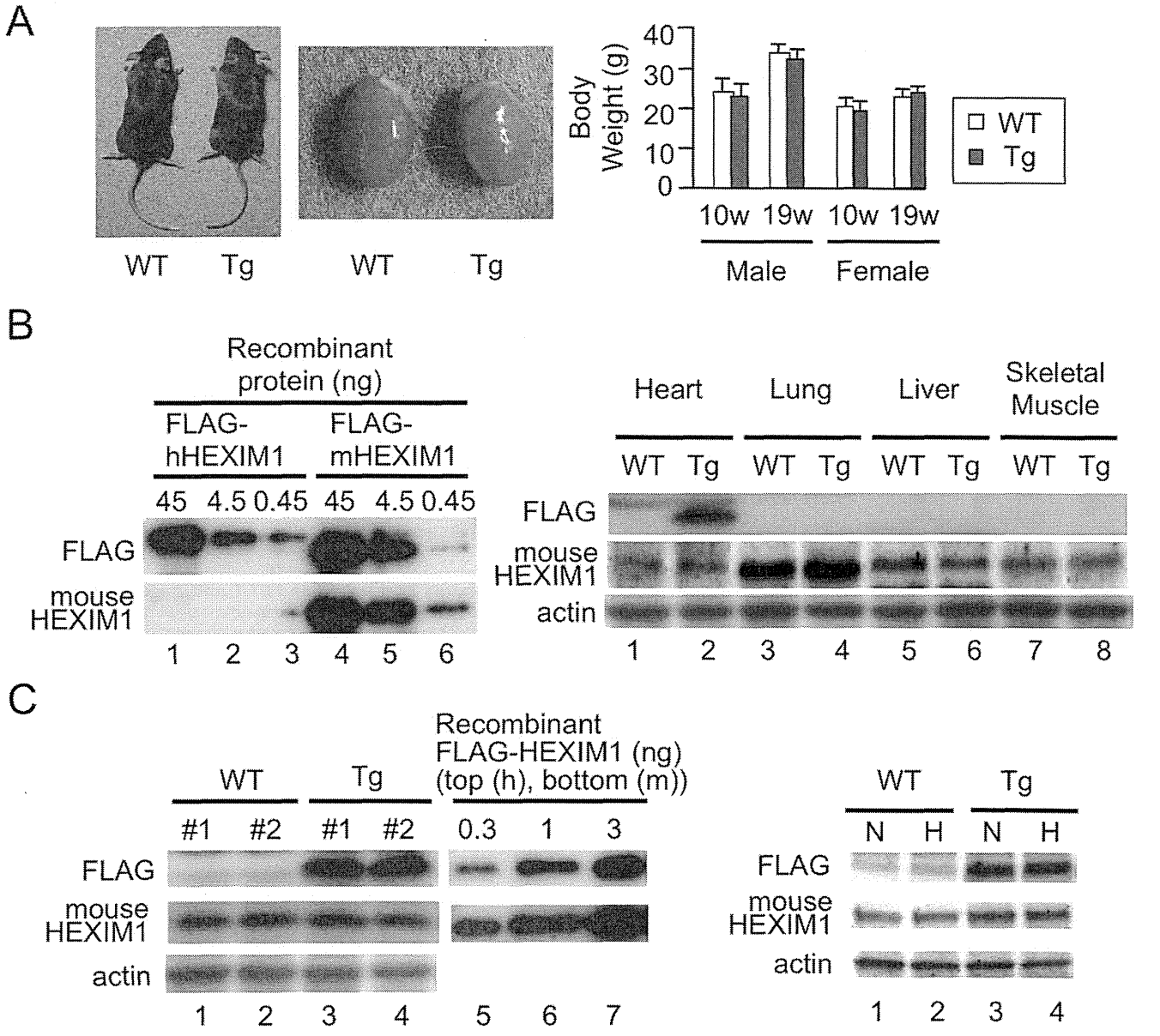

Figure 4. Generation of the transgenic mice with cardiomyocyte-specific overexpression of HEXIM1. (A) Characterization of cardiomyocyte-specific HEXIM1 transgenic (HEX-Tg) mice. *Left*, representative photographs of 19-week-old male WT and HEX-Tg (Tg) mice and their hearts. *Right*, body weight of 10- and 19-week-old WT and HEX-Tg mice. Error bars represent SD (n = 5). (B) Heart-specific expression of FLAG-tagged human HEXIM1 in HEX-Tg mice. *Left*, bacterially expressed purified recombinant FLAG-tagged human and mouse HEXIM1 proteins were analyzed by Western blotting using anti-FLAG antibody or mouse HEXIM1-specific antiserum. *Right*, tissue extracts obtained from heart, lung, liver, and skeletal muscle of WT or HEX-Tg mice were analyzed by Western blotting. (C) Semi-quantification of endogenous and exogenous HEXIM1 protein in WT and HEX-Tg mouse hearts. *Left*, one hundred micrograms of extracts of the hearts from adult WT or HEX-Tg mice and the indicated amounts of bacterially expressed recombinant FLAG-tagged human or mouse HEXIM1 proteins were analyzed by Western blotting. *Right*, endogenous and exogenous HEXIM1 in the heart of WT and HEX-Tg mice exposed to different oxygen conditions were analyzed by Western blotting. N, normoxia. H, hypoxia. In panels B and C, representative images of Western blotting from 5 mice in each condition (genotype and oxygen concentration) and 5 independent experiments are shown.

doi:10.1371/journal.pone.0052522.g004

increases HEXIM1 levels in cardiomyocytes (Fig. 1). Since PGI_2 is known to negatively modulate RV remodeling in experimental PAH animals and PAH patients [45,46], we hypothesized that HEXIM1, most likely via suppression of P-TEFb, takes part in cardiomyocyte regulation in RV.

Despite numerous reports with loss-of-function experiments, it remains unclear whether increase of HEXIM1 expression levels, as a physiological inhibitor of P-TEFb, can exert antihypertrophic effect in cardiomyocytes. Moreover, the role of HEXIM1 and P-TEFb in the progression of RVH remains elusive. Given this, using adenovirus-mediated gene delivery to NRCM, we for the first time confirmed that overexpression of HEXIM1 prevents cardiomyocyte hypertrophy (Fig. 2). Since ET-1 is a well-characterized inducer of cardiomyocyte hypertrophy and shown to induce Ser2 phosphorylation of RNAP II CTD via P-TEFb activation, we tested the effect of overexpression of HEXIM1 on

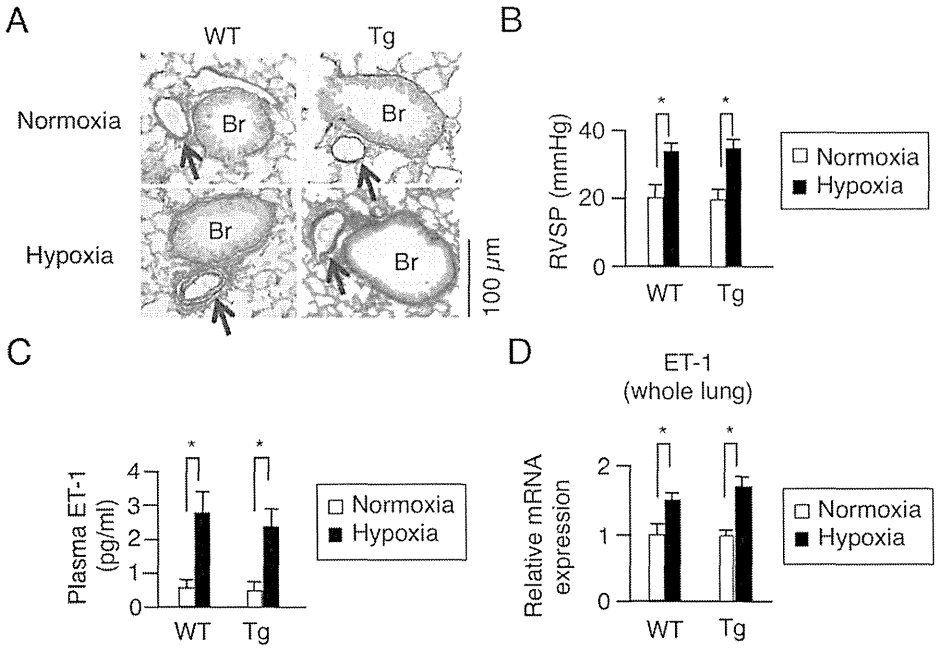

Figure 5. Pathophysiological changes of pulmonary artery, hemodynamic, plasma ET-1 levels, and ET-1 mRNA expression of the lung in a hypoxia-induced pulmonary arterial hypertension model. WT and HEX-Tg (Tg) mice were placed in normoxic or hypoxic conditions for 10 weeks. (A) Pulmonary vascular remodeling in WT and HEX-Tg mice exposed to chronic hypoxia. Representative photographs of Elastica Van Gieson stains of the lung sections of WT and HEX-Tg mice under normoxic and hypoxic conditions are shown (from 10 mice in each condition and genotype). Br, bronchiole. Arrow, pulmonary artery. (B) Right ventricular systolic pressure (RVSP) in WT and HEX-Tg mice exposed to chronic hypoxia. (C) Plasma ET-1 levels in WT and HEX-Tg mice exposed to chronic hypoxia. (D) mRNA expression levels of ET-1 in the whole lung extracts. Total RNA was extracted from lung tissues in each condition (genotype and oxygen concentration), and expression levels of mRNA of ET-1 were assessed in qRT-PCR analysis. Results were normalized to GAPDH mRNA levels and are shown as relative mRNA expression levels in the WT mice placed in normoxic condition. Error bars represent SD (n = 10). *P<0.05.
doi:10.1371/journal.pone.0052522.g005

ET-1-induced cardiomyocyte hypertrophy as a model. We revealed that overexpression of HEXIM1 prevents ET-1-induced Ser2 site-specific phosphorylation of RNAPII and shows anti-hypertrophic effect. Using a HEXIM1 mutant lacking central basic region, which diminishes P-TEFb-suppressing activity and permits Ser2 phosphorylation of CTD, we demonstrated that this HEXIM1 mutant could not suppress ET-1-induced activation of P-TEFb and myocyte hypertrophy (Fig. 2). Together, we may propose that the inhibition of phosphorylation of Ser2 of the CTD via suppression of P-TEFb activity is essential for antihypertrophic effect of HEXIM1 in ET-1-stimulated cardiomyocytes. So far examined, we could not find any effect of HEXIM1 over-expression on the other signaling pathways located downstream of ET-1. These issues are supported by the negative effects of overexpressed HEXIM1 on ET-1-induced mRNA expression of ANP, BNP, beta-MHC, and alpha skeletal muscle actin (Fig. 3), all of which are known to be a representative marker in hypertrophic myocardium and beta-MHC is also known to play a physiological role in cardiac hypertrophy [41,47]. Again, the mutant HEXIM1 lacking suppression activity of P-TEFb did not inhibit ET-1 effect on mRNA expression of those genes. Notably, HEXIM1 did not significantly influence on mRNA expression of type I collagen mRNA expression in cardiomyocytes and on that of type I collagen and ANP in cardiac fibroblasts (Fig. 3), suggesting that negative effect of HEXIM1 might be gene-specific in cardiomyocytes. Since those genes, i.e., ANP, BNP, beta-MHC, and alpha skeletal muscle actin, are known to be under the control of a set of transcription factors including GATA-4 under hypertrophic stimuli [41,48,49], we may consider that HEXIM1 suppresses hypertrophic myocyte growth via inhibition of GATA-4-P-TEFb interaction. Of course, further studies are needed to unveil the underlying mechanism of HEXIM1, since it is shown that HEXIM1 negatively modulates transcription not only via P-TEFb suppression but also via P-TEFb-independent repression of several transcription factors [14,15,18,19].

By crossing the mice heterozygous encoding HEXIM1 preceded by the loxP-flanked stuffer sequence with another mice expressing Cre recombinase under the control of the alpha-MHC promoter, the resultant transgenic mice express HEXIM1 exclusively after birth in cardiomyocytes, eliminating the gene dosage effects of HEXIM1 during fetal period. Our quantitative analysis showed that those transgenic mice express exogenous HEXIM1 at relatively high levels: approximately ten times of endogenous HEXIM1. The appearance of HEX-Tg mice and their hearts was indistinguishable from that of WT mice and their hearts under normoxic conditions. However, under hypoxic conditions, HEX-Tg mice were resistant to RVH without alteration in muscularization of small, normally nonmuscular, arteries in the alveolar walls and systolic pressure in RV (Figs. 4–6). Although the molecular mechanism for RVH under chronic hypoxia is not well understood, previous studies indicated that chronic hypoxia increases plasma levels of ET-1 and enhances GATA-4 activity in the RV [50,51]. Moreover, elevation of circulating levels of ET-1 is reported in PAH patients with RVH [52–54]. Together with the results from our experiments with NRCM, it is suggested that overexpressed HEXIM1 in transgenic mice may contribute to negative regulation of myocyte hypertrophy in RV, at least in part, via intervening ET-1 action. However, two important questions remain to be addressed; why HEX-Tg mice does not show phenotypic alteration in LV, and why CLP-

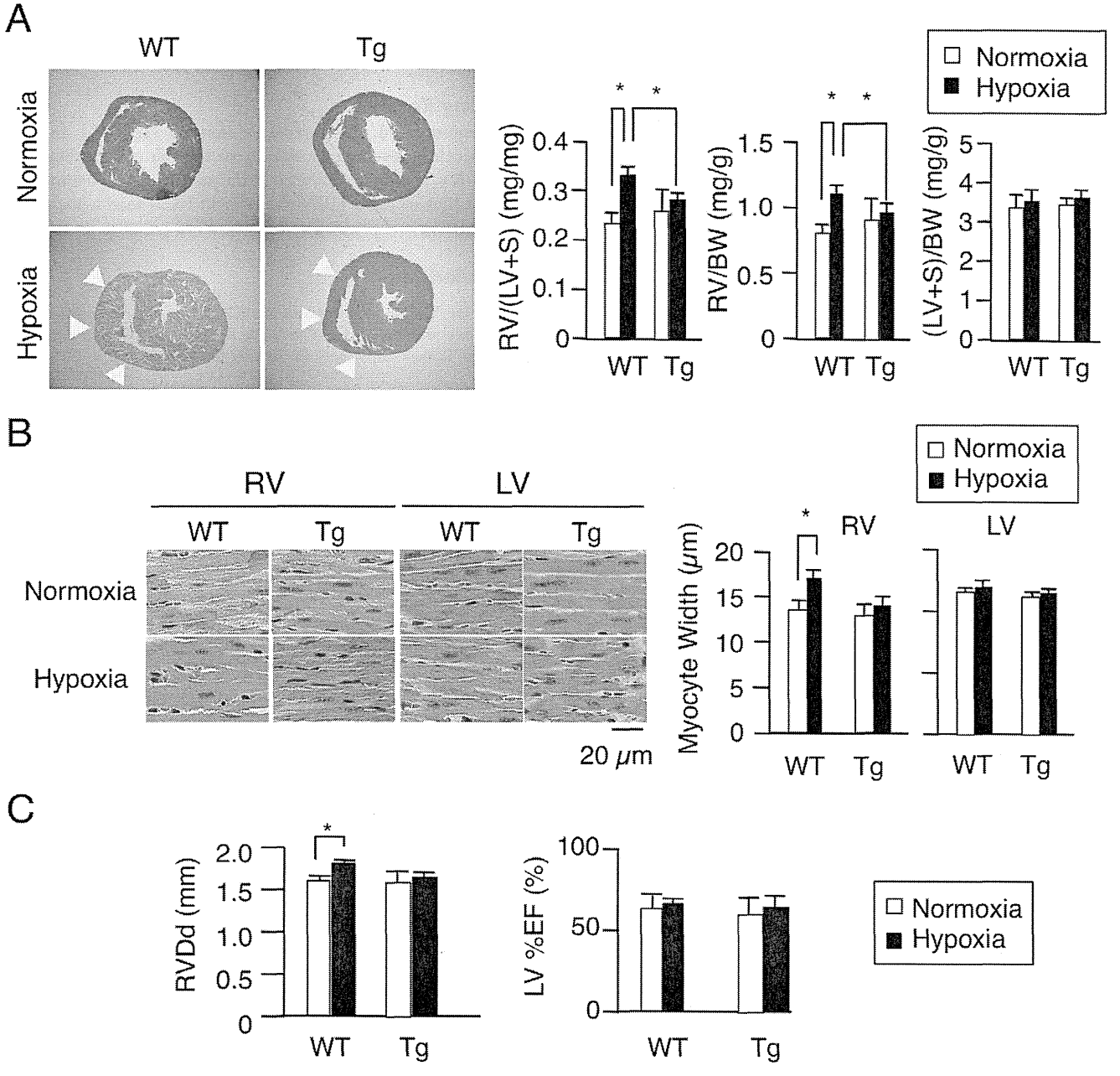

Figure 6. Cardiomyocyte-specific overexpression of HEXIM1 attenuates right ventricular hypertrophy in a hypoxia-induced PAH model. WT and HEX-Tg (Tg) mice were placed in normoxic or hypoxic conditions for 10 weeks. (A) Effect of HEXIM1 on the development of RVH in mice exposed to chronic hypoxia. *Left*, representative photographs of cross-sections of the hearts stained with Hematoxylin-Eosin solution from 10 mice in each condition (genotype and oxygen concentration) are shown. *Right*, assessment of the RV weight to LV+S weight (RV/(LV+S)), RV weight to body weight (RV/BW), and LV+S weight to BW ((LV+S)/BW) are shown. Arrows, RV wall. (B) Effect of HEXIM1 on cardiomyocyte hypertrophy in mice exposed to chronic hypoxia. *Left*, representative photographs of Hematoxylin and Eosin stains of RV and LV sections of WT and HEX-Tg mice under normoxic and hypoxic conditions are shown. *Right*, 200 myocytes in each condition (genotype and oxygen concentration) were counted in randomly selected fields and myocyte width was measured. (C) Right ventricular end-diastolic diameter (RVDd) and ejection fraction of left ventricle (LV%EF) measured by ultrasound cardiography. Error bars represent SD (n = 10). *P<0.05.
doi:10.1371/journal.pone.0052522.g006

$1^{-/-}$ mice do not have RV abnormality. Interestingly, it is reported that not CLP-$1^{+/-}$ but alphaMHC–cyclin T1/CLP-$1^{+/-}$ double transgenic mice exhibited enhanced susceptibility to LVH [23]. We, at this moment, do not have the answer to these questions, but we have to consider as yet unidentified mechanism for myocyte size regulation that is also intervened by HEXIM1. Since only a small portion of HEXIM1 is sequestered in P-TEFb complex, HEXIM1 might interact with other signaling pathways in cardiomyocytes. Indeed, we and the others previously reported that HEXIM1 interacts with several transcription factors independently from 7SK snRNA and P-TEFb [15,18,19]. For example, there was a significant increase in the levels of HIF-1alpha protein in CLP-$1^{+/-}$ hearts subjected to ischemic stress as compared to CLP-$1^{+/+}$ hearts [26], suggesting that HEXIM1

might prevent the activation of HIF-1 pathway. Moreover, HEXIM1 could modulate TGF-beta1/Smad3 and Jak/STAT signaling pathway [24]. In any case, it appears evident that HEXIM1 plays a pivotal role in myocyte size regulation in RV under chronic hypoxia and PAH. Although the cause of RV dysfunction and the feasibility of therapeutically targeting the RVH are uncertain, RV dilatation was observed in WT mice but not in HEX-Tg mice under chronic hypoxia (Fig. 6C), suggesting that therapies that target RVH by HEXIM1 might be beneficial in PAH.

As previously described, PGIS is reduced in PAH patients, resulting in reduced production of PGI_2 [55]. Based on this, PGI_2 is therapeutically administered in PAH patients and its clinical benefits are well documented [56]. Of note, PGI_2 is shown to not only act as a vasodilator but also have antiproliferative effects [37,45]. HMBA is reported to induce HEXIM1 expression and show antiproliferative effects in vascular smooth muscle cells [57]. Although it is not clear whether HEXIM1 expression is induced by PGI_2 in vivo and therapeutic effect of PGI_2 is mediated by HEXIM1, we showed that PGI_2 increases HEXIM1 protein levels and introduction of siRNA against HEXIM1 cancelled anti-hypertrophic effect of PGI_2, at least, in cultured cardiomyocytes (Fig. 1). In this line, it might be extremely interesting to further address molecular mechanism of therapeutic effects of PGI_2 in PAH. HEXIM1 inducer, if pharmacologically developed, might act as a novel therapeutic bullet in PAH.

Concluding Remarks

We demonstrated that overexpression of HEXIM1 in the cardiomyocytes prevents hypertrophy in the cultured cardiomyocytes and RV in hypoxia-induced PAH model mice. Therapeutic modalities that increase HEXIM1 protein levels might intervene RV remodeling and prolong survival in PAH patients.

Acknowledgments

We thank Dr. Tadashi Tanabe and Dr. Kinya Otsu for providing PGIS deficient mice and alphaMHC-Cre mice, respectively. We also thank all members of Tanaka Laboratory for helpful comments.

Author Contributions

Conceived and designed the experiments: NY NS MS HT. Performed the experiments: NY NS T. Maruyama T. Matsuhashi MK HO T. Sawai. Analyzed the data: NY NS MS KF T. Satoh HT. Contributed reagents/materials/analysis tools: NY NS MS AK OH CM HT. Wrote the paper: NY NS HT.

References

1. McLaughlin VV, Archer SL, Badesch DB, Barst RJ, Farber HW, et al. (2009) ACCF/AHA 2009 expert consensus document on pulmonary hypertension a report of the American College of Cardiology Foundation Task Force on Expert Consensus Documents and the American Heart Association developed in collaboration with the American College of Chest Physicians; American Thoracic Society, Inc.; and the Pulmonary Hypertension Association. J Am Coll Cardiol 53: 1573–1619.
2. Archer SL, Weir EK, Wilkins MR (2010) Basic science of pulmonary arterial hypertension for clinicians: new concepts and experimental therapies. Circulation 121: 2045–2066.
3. Michelakis ED, Wilkins MR, Rabinovitch M (2008) Emerging concepts and translational priorities in pulmonary arterial hypertension. Circulation 118: 1486–1495.
4. Haddad F, Doyle R, Murphy DJ, Hunt SA (2008) Right ventricular function in cardiovascular disease, part II: pathophysiology, clinical importance, and management of right ventricular failure. Circulation 117: 1717–1731.
5. Bogaard HJ, Abe K, Vonk Noordegraaf A, Voelkel NF (2009) The right ventricle under pressure: cellular and molecular mechanisms of right-heart failure in pulmonary hypertension. Chest 135: 794–804.
6. Esposito G, Rapacciuolo A, Naga Prasad SV, Takaoka H, Thomas SA, et al. (2002) Genetic alterations that inhibit in vivo pressure-overload hypertrophy prevent cardiac dysfunction despite increased wall stress. Circulation 105: 85–92.
7. Gardin JM, Lauer MS (2004) Left ventricular hypertrophy: the next treatable, silent killer? JAMA 292: 2396–2398.
8. Wilkins MR, Paul GA, Strange JW, Tunariu N, Gin-Sing W, et al. (2005) Sildenafil versus Endothelin Receptor Antagonist for Pulmonary Hypertension (SERAPH) study. Am J Respir Crit Care Med 171: 1292–1297.
9. Archer SL, Michelakis ED (2009) Phosphodiesterase type 5 inhibitors for pulmonary arterial hypertension. N Engl J Med 361: 1864–1871.
10. Piao L, Fang YH, Cadete VJ, Wietholt C, Urboniene D, et al. (2010) The inhibition of pyruvate dehydrogenase kinase improves impaired cardiac function and electrical remodeling in two models of right ventricular hypertrophy: resuscitating the hibernating right ventricle. J Mol Med (Berl) 88: 47–60.
11. Kusuhara M, Nagasaki K, Kimura K, Maass N, Manabe T, et al. (1999) Cloning of hexamethylene-bis-acetamide-inducible transcript, HEXIM1, in human vascular smooth muscle cells. Biomed Res 20: 273–279.
12. Zhou Q, Yik JH (2006) The Yin and Yang of P-TEFb regulation: implications for human immunodeficiency virus gene expression and global control of cell growth and differentiation. Microbiol Mol Biol Rev 70: 646–659.
13. Peterlin BM, Price DH (2006) Controlling the elongation phase of transcription with P-TEFb. Mol Cell 23: 297–305.
14. Wittmann BM, Fujinaga K, Deng H, Ogba N, Montano MM (2005) The breast cell growth inhibitor, estrogen down regulated gene 1, modulates a novel functional interaction between estrogen receptor alpha and transcriptional elongation factor cyclin T1. Oncogene 24: 5576–5588.
15. Shimizu N, Ouchida R, Yoshikawa N, Hisada T, Watanabe H, et al. (2005) HEXIM1 forms a transcriptionally abortive complex with glucocorticoid receptor without involving 7SK RNA and positive transcription elongation factor b. Proc Natl Acad Sci U S A 102: 8555–8560.
16. Yoshikawa N, Shimizu N, Sano M, Ohnuma K, Iwata S, et al. (2008) Role of the hinge region of glucocorticoid receptor for HEXIM1-mediated transcriptional repression. Biochem Biophys Res Commun 371: 44–49.
17. Shimizu N, Yoshikawa N, Wada T, Handa H, Sano M, et al. (2008) Tissue- and context-dependent modulation of hormonal sensitivity of glucocorticoid-responsive genes by hexamethylene bisacetamide-inducible protein 1. Mol Endocrinol 22: 2609–2623.
18. Montano MM, Doughman YQ, Deng H, Chaplin L, Yang J, et al. (2008) Mutation of the HEXIM1 gene results in defects during heart and vascular development partly through downregulation of vascular endothelial growth factor. Circ Res 102: 415–422.
19. Ouchida R, Kusuhara M, Shimizu N, Hisada T, Makino Y, et al. (2003) Suppression of NF-kappaB-dependent gene expression by a hexamethylene bisacetamide-inducible protein HEXIM1 in human vascular smooth muscle cells. Genes Cells 8: 95–107.
20. Sano M, Abdellatif M, Oh H, Xie M, Bagella L, et al. (2002) Activation and function of cyclin T-Cdk9 (positive transcription elongation factor-b) in cardiac muscle-cell hypertrophy. Nat Med 8: 1310–1317.
21. Huang F, Wagner M, Siddiqui MA (2004) Ablation of the CLP-1 gene leads to down-regulation of the HAND1 gene and abnormality of the left ventricle of the heart and fetal death. Mech Dev 121: 559–572.
22. Espinoza-Derout J, Wagner M, Shahmiri K, Mascareno E, Chaqour B, et al. (2007) Pivotal role of cardiac lineage protein-1 (CLP-1) in transcriptional elongation factor P-TEFb complex formation in cardiac hypertrophy. Cardiovasc Res 75: 129–138.
23. Espinoza-Derout J, Wagner M, Salciccioli L, Lazar JM, Bhaduri S, et al. (2009) Positive transcription elongation factor b activity in compensatory myocardial hypertrophy is regulated by cardiac lineage protein-1. Circ Res 104: 1347–1354.
24. Mascareno E, Galatioto J, Rozenberg I, Salciccioli L, Kamran H, et al. (2012) Cardiac lineage protein-1 (CLP-1) regulates cardiac remodeling via transcriptional modulation of diverse hypertrophic and fibrotic responses and angiotensin II-transforming growth factor β (TGF-β1) signaling axis. J Biol Chem 287: 13084–13093.
25. Ogba N, Doughman YQ, Chaplin LJ, Hu Y, Gargesha M, et al. (2010) HEXIM1 modulates vascular endothelial growth factor expression and function in breast epithelial cells and mammary gland. Oncogene 29: 3639–3649.
26. Mascareno E, Manukyan I, Das DK, Siddiqui MA (2009) Down-regulation of cardiac lineage protein (CLP-1) expression in CLP-1+/− mice affords. J Cell Mol Med 13: 2744–2753.
27. Uzuki M, Sasano H, Muramatsu Y, Totsune K, Takahashi K, et al. (2001) Urocortin in the synovial tissue of patients with rheumatoid arthritis. Clin Sci (Lond) 100: 577–589.
28. Yokoyama C, Yabuki T, Shimonishi M, Wada M, Hatae T, et al. (2002) Prostacyclin-deficient mice develop ischemic renal disorders, including nephrosclerosis and renal infarction. Circulation 106: 2397–2403.
29. Nishida K, Yamaguchi O, Hirotani S, Hikoso S, Higuchi Y, et al. (2004) p38alpha mitogen-activated protein kinase plays a critical role in cardiomyocyte survival but not in cardiac hypertrophic growth in response to pressure overload. Mol Cell Biol 24: 10611–10620.

30. Shimizu N, Yoshikawa N, Ito N, Maruyama T, Suzuki Y, et al. (2011) Crosstalk between glucocorticoid receptor and nutritional sensor mTOR in skeletal muscle. Cell Metab 13: 170–182.
31. Yoshikawa N, Nagasaki M, Sano M, Tokudome S, Ueno K, et al. (2009) Ligand-based gene expression profiling reveals novel roles of glucocorticoid receptor in cardiac metabolism. Am J Physiol Endocrinol Metab 296: E1363–1373.
32. Endo J, Sano M, Fujita J, Hayashida K, Yuasa S, et al. (2007) Bone marrow derived cells are involved in the pathogenesis of cardiac hypertrophy in response to pressure overload. Circulation 116: 1176–1184.
33. Unverferth DV, Baker PB, Swift SE, Chaffee R, Fetters JK, et al. (1986) Extent of myocardial fibrosis and cellular hypertrophy in dilated cardiomyopathy. Am J Cardiol 57: 816–820.
34. Huang F, Wagner M, Siddiqui MA (2002) Structure, expression, and functional characterization of the mouse CLP-1 gene. Gene 292: 245–259.
35. Turano M, Napolitano G, Dulac C, Majello B, Bensaude O, et al. (2006) Increased HEXIM1 expression during erythroleukemia and neuroblastoma cell differentiation. J Cell Physiol 206: 603–610.
36. Contreras X, Barboric M, Lenasi T, Peterlin BM (2007) HMBA releases P-TEFb from HEXIM1 and 7SK snRNA via PI3K/Akt and activates HIV transcription. PLoS Pathog 3: 1459–1469.
37. Ritchie RH, Rosenkranz AC, Huynh LP, Stephenson T, Kaye DM, et al. (2004) Activation of IP prostanoid receptors prevents cardiomyocyte hypertrophy via cAMP-dependent signaling. Am J Physiol Heart Circ Physiol 287: H1179–1185.
38. Schermuly RT, Kreisselmeier KP, Ghofrani HA, Samidurai A, Pullamsetti S, et al. (2004) Antiremodeling effects of iloprost and the dual-selective phosphodiesterase 3/4 inhibitor tolafentrine in chronic experimental pulmonary hypertension. Circ Res 94: 1101–1108.
39. Sugden PH (2003) An overview of endothelin signaling in the cardiac myocyte. J Mol Cell Cardiol 35: 871–886.
40. Wang L, Proud CG (2002) Ras/Erk signaling is essential for activation of protein synthesis by Gq protein-coupled receptor agonists in adult cardiomyocytes. Circ Res 91: 821–829.
41. Rohini A, Agrawal N, Koyani CN, Singh R (2010) Molecular targets and regulators of cardiac hypertrophy. Pharmacol Res 61: 269–280.
42. Stenmark KR, Meyrick B, Galie N, Mooi WJ, McMurtry IF (2009) Animal models of pulmonary arterial hypertension: the hope for etiological discovery and pharmacological cure. Am J Physiol Lung Cell Mol Physiol 297: L1013–1032.
43. Mizuno S, Bogaard HJ, Kraskauskas D, Alhussaini A, Gomez-Arroyo J, et al. (2011) p53 Gene deficiency promotes hypoxia-induced pulmonary hypertension and vascular remodeling in mice. Am J Physiol Lung Cell Mol Physiol 300: L753–761.
44. Haddad F, Hunt SA, Rosenthal DN, Murphy DJ (2008) Right ventricular function in cardiovascular disease, part I: Anatomy, physiology, aging, and functional assessment of the right ventricle. Circulation 117: 1436–1448.
45. Roeleveld RJ, Vonk-Noordegraaf A, Marcus JT, Bronzwaer JG, Marques KM, et al. (2004) Effects of epoprostenol on right ventricular hypertrophy and dilatation in pulmonary hypertension. Chest 125: 572–579.
46. Obata H, Sakai Y, Ohnishi S, Takeshita S, Mori H, et al. (2008) Single injection of a sustained-release prostacyclin analog improves pulmonary hypertension in rats. Am J Respir Crit Care Med 177: 195–201.
47. Krenz M, Robbins J (2004) Impact of beta-myosin heavy chain expression on cardiac function during stress. J Am Coll Cardiol 44: 2390–2397.
48. Akazawa H, Komuro I (2003) Roles of cardiac transcription factors in cardiac hypertrophy. Circ Res 92: 1079–1088.
49. Liang Q, Molkentin JD (2002) Divergent signaling pathways converge on GATA4 to regulate cardiac hypertrophic gene expression. J Mol Cell Cardiol 34: 611–616.
50. Yamashita K, Discher DJ, Hu J, Bishopric NH, Webster KA (2001) Molecular regulation of the endothelin-1 gene by hypoxia. Contributions of hypoxia-inducible factor-1, activator protein-1, GATA-2, AND p300/CBP. J Biol Chem 276: 12645–12653.
51. Park AM, Wong CM, Jelinkova L, Liu L, Nagase H, et al. (2010) Pulmonary hypertension-induced GATA4 activation in the right ventricle. Hypertension 56: 1145–1151.
52. Stewart DJ, Levy RD, Cernacek P, Langleben D (1991) Increased plasma endothelin-1 in pulmonary hypertension: marker or mediator of disease? Ann Intern Med 114: 464–469.
53. Filep JG, Bodolay E, Sipka S, Gyimesi E, Csipö I, et al. (1995) Plasma endothelin correlates with antiendothelial antibodies in patients with mixed connective tissue disease. Circulation 92: 2969–2974.
54. Nootens M, Kaufmann E, Rector T, Toher C, Judd D, et al. (1995) Neurohormonal activation in patients with right ventricular failure from pulmonary hypertension: relation to hemodynamic variables and endothelin levels. J Am Coll Cardiol 26: 1581–1585.
55. Tuder RM, Cool CD, Geraci MW, Wang J, Abman SH, et al. (1999) Prostacyclin synthase expression is decreased in lungs from patients with severe pulmonary hypertension. Am J Respir Crit Care Med 159: 1925–1932.
56. Barst RJ, Gibbs JS, Ghofrani HA, Hoeper MM, McLaughlin VV, et al. (2009) Updated evidence-based treatment algorithm in pulmonary arterial hypertension. J Am Coll Cardiol 54: S78–84.
57. Grainger DJ, Hesketh TR, Weissberg PL, Metcalfe JC (1992) Hexamethylene-bisacetamide selectively inhibits the proliferation of human and rat vascular smooth-muscle cells. Biochem J 283 (Pt 2): 403–408.

Clinical Cancer Research

Impact of the Integrin Signaling Adaptor Protein NEDD9 on Prognosis and Metastatic Behavior of Human Lung Cancer

Shunsuke Kondo[1], Satoshi Iwata[2], Taketo Yamada[4], Yusuke Inoue[7], Hiromi Ichihara[3], Yoshiko Kichikawa[2], Tomoki Katayose[2], Akiko Souta-Kuribara[2], Hiroto Yamazaki[2], Osamu Hosono[2], Hiroshi Kawasaki[2], Hirotoshi Tanaka[2], Yuichiro Hayashi[4], Michiie Sakamoto[4], Kazunori Kamiya[5], Nam H. Dang[8], and Chikao Morimoto[6]

Abstract

Purpose: In a substantial population of non–small cell lung cancer (NSCLC), expression and activation of EGF receptor (EGFR) have been reported and is regarded as a novel molecular target. A growing body of evidence has shown the signaling crosstalk between EGFR and integrins in cellular migration and invasion. NEDD9 is an integrin signaling adaptor protein composed of multiple domains serving as substrate for a variety of tyrosine kinases. In the present study, we aimed at elucidating a role of NEDD9 in the signaling crosstalk between EGFR and integrins.

Experimental Design: Using NSCLC cell lines, we conducted immunoblotting and cellular migration/invasion assay *in vitro*. Next, we analyzed metastasis assays *in vivo* by the use of xenograft transplantation model. Finally, we retrospectively evaluated clinical samples and records of patients with NSCLCs.

Results: We showed that tyrosine phosphorylation of NEDD9 was reduced by the inhibition of EGFR in NSCLC cell lines. Overexpression of constitutively active EGFR caused tyrosine phosphorylation of NEDD9 in the absence of integrin stimulation. By gene transfer and gene knockdown, we showed that NEDD9 plays a pivotal role in cell migration and invasion of those cells *in vitro*. Furthermore, overexpression of NEDD9 promoted lung metastasis of an NSCLC cell line in NOD/Shi-scid, IL-2Rγ^{null} mice (NOG) mice. Finally, univariate and multivariate Cox model analysis of NSCLC clinical specimens revealed a strong correlation between NEDD9 expression and recurrence-free survival as well as overall survival.

Conclusion: Our data thus suggest that NEDD9 is a promising biomarker for the prognosis of NSCLCs and its expression can promote NSCLC metastasis. *Clin Cancer Res; 18(22); 6326–38. ©2012 AACR.*

Introduction

Lung cancer is the leading cause of cancer-related mortality in men worldwide (1). Non–small cell lung cancer (NSCLC) constitutes more than 80% of lung cancer, whereas small cell lung cancer being around 13%. While surgical intervention is the therapeutic option in limited stage NSCLCs, relapse rate is very high, being around 40% within 5 years after surgical intervention with curative intent. Moreover, the prevalence rate of NSCLCs continues to grow, and 5-year survival rate after diagnosis is only 15% to 25%.

Large randomized trials showed that platinum-based adjuvant chemotherapy has modest survival advantage (HR, 0.6–0.8) for carefully selected patients with NSCLCs (2). Prognostic factor is a powerful tool to determine patients who may benefit from adjuvant chemotherapy, as well as the type of treatments which may benefit the patients. Besides tumor–node–metastasis (TNM) staging, which is the most important clinical prognostic factor for NSCLCs, several studies have examined gene expression profiles of NSCLCs, identifying molecular subtypes associated with patient outcome.

The EGF receptor (EGFR)/human epidermal receptor (HER) 1 is one such gene signature which has received increasing attention over the last decade. EGFR is a receptor tyrosine kinase (RTK; ref. 3) that frequently is overexpressed or harbors constitutively active mutations in NSCLCs. Its activation promotes tumor proliferation, invasion, and metastasis (4). The small molecule tyrosine kinase inhibitors (TKI) gefitinib and erlotinib target the ATP-binding

Authors' Affiliations: [1]Hepatobiliary and Pancreatic Oncology Division, National Cancer Center Hospital; [2]Department of Rheumatology and Allergy, Research Hospital, [3]Division of Molecular Pathology, The Institute of Medical Science, The University of Tokyo; [4]Department of Pathology, School of Medicine, [5]Department of Pathology and Department of Surgery, Division of General Thoracic Surgery, School of Medicine, Keio University; [6]Department of Therapy Development and Innovation for Immune Disorders and Cancers, Graduate School of Medicine, Juntendo University, Tokyo; [7]Department of Diagnostic Radiology, Kitasato University Hospital, Kanagawa, Japan; and [8]Division of Hematology and Oncology, University of Florida Shands Cancer Center, Gainesville, Florida

Note: Supplementary data for this article are available at Clinical Cancer Research Online (http://clincancerres.aacrjournals.org/).

Corresponding Author: Chikao Morimoto, Department of Therapy Development and Innovation for Immune Disorders and Cancers, Graduate School of Medicine, Juntendo University, 2-1-1, Hongo, Bunkyo-ku, Tokyo 113-8421, Japan. Phone: 81-3-3868-2310; Fax: 81-3-3868-2310; E-mail: morimoto@ims.u-tokyo.ac.jp

doi: 10.1158/1078-0432.CCR-11-2162

©2012 American Association for Cancer Research.

Translational Relevance

EGF receptor (EGFR) is regarded as a novel molecular target in non–small cell lung cancer (NSCLC). In this study, we focused on the interaction of NEDD9 and EGFR, as NEDD9 is a docking protein downstream of β1-integrins, which closely associates with EGFR. We showed the following findings.

1. EGFR is involved in tyrosine phosphorylation of NEDD9.
2. NEDD9 mediates EGFR-/β1-integrin–induced migration and invasion of NSCLC cell lines.
3. In a murine xenograft model, NEDD9 promotes lung metastasis of an NSCLC cell line.
4. NEDD9 expression in primary lesion of NSCLCs strongly correlates with recurrence-free survival or overall survival of the patients with NSCLCs.

Our results suggest that NEDD9 is a useful biomarker for the prognosis of NSCLCs, and its expression can promote NSCLC metastasis.

This is the first study to show the clinical importance of NEDD9 as a potential prognostic factor as well as the crosstalk between EGFR and NEDD9 signaling pathways in NSCLCs.

pocket of EGFR and subsequent signal transduction (5), with recent studies showing a correlation between clinical effectiveness of gefitinib in NSCLCs and specific EGFR-activating mutation (6, 7).

Recent work showed crosstalk of signaling pathways between the integrin family of adhesion molecules and RTKs in cancer metastasis and invasion (8–10). Integrins contribute to migration and invasion of cancer cells (11, 12), and elevated β1-integrin expression affects NSCLC prognosis. While integrins and EGFR may potentially regulate each other in a reciprocal manner, key molecules involved in this signaling crosstalk that can influence NSCLC tumorigenesis, metastasis, and prognosis remain to be identified.

We initially identified pp105 as the major phosphotyrosine-containing protein in H9 T-cell line stimulated with β1-integrins (13, 14). Sequence analysis of isolated cDNA clone revealed homology with p130 Crk-associated substrate (Cas)/breast cancer anti-estrogen resistance 1 (*BCAR1*: gene symbol) which was identified as a tyrosine-phosphorylated protein in v-Crk and v-Src–transformed fibroblasts (15), thus designating pp105 as Crk-associated substrate lymphocyte type (Cas-L). Cas-L is identical to neural precursor cell–expressed, developmentally downregulated 9 (NEDD9: gene symbol; ref. 16) and human enhancer of filamentation 1 (HEF1; ref. 17). NEDD9/HEF1/Cas-L is an integrin signaling adaptor or docking protein that consists of multiple preserved domains common to Cas family members (18).

NEDD9 is phosphorylated at its tyrosine residues by integrins and other stimuli. Ligation of T- and B-cell antigen receptors (19, 20) caused tyrosine phosphorylation of NEDD9, resulting in the association of Crk, Crk-L, and C3G. Integrin- or integrin/TCR-elicited tyrosine phosphorylation of NEDD9 was mediated by focal adhesion kinase (FAK) and Src family tyrosine kinases (21, 22). Ectopic expression of NEDD9 conferred T cells with enhanced motility on the co-engagement of TCR/CD3 complex and β1-integrins (23, 24), suggesting a pivotal role of tyrosine-phosphorylated NEDD9 in TCR- and integrin-mediated cell motility. Recent work showed that NEDD9 expression correlates with metastatic behavior of several malignancies, including lung cancer, head and neck cancer, melanoma, and breast cancer (25–31).

In this study, we investigated the biologic significance of the link between NEDD9 and EGFR signaling pathway in NSCLCs by *in vitro* and *in vivo* approaches. Furthermore, we evaluated the clinical significance of NEDD9 expression in primary NSCLC tumor samples through a retrospective analysis. We showed that NEDD9 plays a pivotal role in cell metastasis and invasion of NSCLC cells, and expression of NEDD9 appears to be a promising biomarker for NSCLC prognosis.

Materials and Methods

Reagents and antibodies

Gefitinib was purchased from Biaffin GmbH & Co KG. Recombinant human EGF was purchased from R&D systems, Inc. Monoclonal antibodies (mAb) against FAK and BCAR1 were purchased from BD. Rabbit anti-phospho-FAK (Tyr-397) polyclonal antibody (pAb) was from Invitrogen. Mouse mAb against NEDD9 (2G9) was purchased from ImmuQuest Ltd. Rabbit pAb against NEDD9 was produced by MBL by immunizing synthetic peptide EYPSRYQKDVY-DIPPSH. Anti-phosphotyrosine antibody (4G10) and anti-c-myc tag mAb (9E10) were produced from the hybridoma obtained from American Type Culture Collection. Anti-EGFR pAb, anti-phospho-EGFR (Tyr-1068) pAb, and anti-β-actin mAb were from Cell Signaling Technology, Inc. All chemicals were purchased from Sigma-Aldrich unless otherwise stated.

Cells, plasmids, and transfection procedures

293T cells and A549 cells were obtained from American Type Culture Collection. PC-9 cells harboring the gefitinib-sensitizing deletion mutation (ΔE746-A750) and PC-14 were kindly provided by Dr. F. Koizumi (National Cancer Center Hospital, Tokyo, Japan) and were maintained as described previously (32).

The plasmid vector pBabe puro EGFR wild-type and its constitutively active mutants EGFR (del3) L747-E749del, A750P, EGFR G719S, EGFR D770-N771 insNPG, EGFR L858R, and its kinase dead mutant EGFR D837A were described previously (33). The plasmid vector pSRα c-myc tagged NEDD9 WT (wild-type) was used for transient expression. For stable expression, the following vectors were used: BCMG hygro c-myc NEDD9 WT (wild-type), NEDD9

ΔSH3 (lacking aa 1–60), NEDD9 ΔSD (lacking aa 63–401), NEDD9 ΔC (lacking aa 406–834), NEDD9 ΔYDYVHL (lacking aa 629–834), NEDD9 ΔCC (lacking aa 637–834), NEDD9 ΔHLH (lacking aa 707–834), and NEDD9 F in which Y629 and Y631 were mutated into F. The plasmids were transfected into cells using Lipofectamine 2000 (Invitrogen) or FuGENE6 (Roche Applied Science) according to the manufacturer's instructions. In experiments using BCMG hygro vectors, transfected cells were selected in 0.2 mg/mL hygromycin B to establish stable transformants. The expression vector pMX-luc/neo for firefly luciferase was described elsewhere (34).

Gene knockdown by siRNA

To deplete endogenous NEDD9 or BCAR1, Stealth RNAi siRNAs were obtained from Life Technologies. The target sequence of siRNA for NEDD9 is 5′-UCCCAUGCAGGAGACUGCCUCCAGU-3′ and that for BCAR1 is 5′-GCCUCAAGAUCUUGGUGGGCAUGUA-3′. As a control, we used Stealth RNAi siRNA negative control. The siRNAs were transfected using Lipofectamine RNAiMAX transfection reagent according to the manufacturer's instructions (Life Technologies).

Protein extraction, immunoprecipitation, and immunoblotting

Cells were serum-starved for 24 hours before the treatment with EGF (at a final concentration of 10 ng/mL). For suspension culture, HydroCell low cell binding culture dish (CellSeed Inc.) was used with serum-free medium. Cytoplasmic protein extracts were prepared by detergent lysis (1% Triton X-100) containing phosphatase and protease inhibitors. For immunoprecipitation, cell lysates were incubated with the appropriate first antibody at 4°C overnight and then with protein A Sepharose beads for 4 hours. After wash with lysis buffer, the beads were boiled in the SDS-PAGE loading buffer. The immunoprecipitates and cell lysates were separated by 8% SDS-PAGE gels and electrophoretically transferred onto polyvinylidene difluoride membranes. After blocking, the membranes were incubated serially with the primary antibody and horseradish peroxidase (HRP)-conjugated secondary antibody and then developed by enhanced chemiluminescence system (GE Healthcare).

Cell migration and invasion assays

Cell migration assay was conducted as described previously using Transwell inserts (8-μm pore size; Corning Incorporated; ref. 24). Cells were placed in the upper chamber at 1×10^5 cells/mL in 100 μL of 0.6% bovine serum albumin (BSA)/RPMI-1640 medium. After 6 hours, the inserts were fixed and stained with Diff-Quick. The cells that had not migrated were removed from the upper surface of the inserts using cotton swabs. Images of 3 different high-power fields were captured from each insert, and the number of migratory cells was counted. To determine invasive potential, Matrigel invasion chamber (BD BioCoat) was used.

Animals

Five- to 6-week-old female NOD/Shi-scid, IL-2Rγ^{null} mice (NOG mice; ref. 35) were supplied from Central Institute for Experimental Animals (Kawasaki, Japan) and maintained in a specific pathogen-free facility. All experiments were approved by and carried out following the guidelines of the Institute Animal Care and Use Committee of the University of Tokyo (Tokyo, Japan).

In vivo bioluminescence imaging

Human NSCLC cell line PC-14 was transplanted subcutaneously into the lumbar region on the dorsal side of NOG mice. On days 21 and 28, progression of the transplanted tumors was monitored by the following bioluminescence imaging (BLI) technique. D-Luciferin (Beetle Luciferin Potassium Salt; Promega) was used as the substrate for the luciferase expressed by PC-14 cells. The mice received an intraperitoneal injection of 150 mg/kg D-luciferin and placed in the light tight chamber of a cooled CCD camera system (IVIS Imaging System 100; Xenogen) in the prone position under isoflurane anesthesia. Dorsal, left lateral, ventral, and right lateral images were acquired from 10 minutes after D-luciferin injection with the CCD camera system. All luminescent images were collected with an exposure time of 1 minute and binning of 8.

Gross and microscopic pathology

The NOG mice undergoing xenograft transplantation were euthanized with carbon dioxide on day 28 after BLI. Major organs were examined for grossly visible changes. Lung tissues and the primary tumors were removed into 10% neutral-buffered formalin for histology. After formalin fixation, samples were processed into paraffin wax, sectioned at a nominal thickness of 5 μm, stained with hematoxylin and eosin (H&E), and examined by light microscopy.

Clinical specimens and immunohistochemical staining

Upon approval from the Institutional Review Board of Keio University (Tokyo, Japan), we selected 60 consecutive patients with lung adenocarcinoma treated with curative surgery resection between 1999 and 2001 from the Keio University Hospital (IRB number: 16–90). Immunohistochemical studies were conducted on 5-μm sections of formalin-fixed, paraffin-embedded tissue section of the primary tumors of lung. Antigen retrieval was conducted with 0.01 mol/L of boiled citrate buffer (pH 9.0) for 10 minutes. The slides were stained on the Dako Autostainer (Dako) using the EnVision (Dako) staining reagents. The sections were first blocked for endogenous protein binding and peroxidase activity with Dual Endogenous Block (Dako) for 10 minutes. The sections were serially incubated with a polyclonal antibody against NEDD9 (2 μg/mL) and EnVision+ Dual Link reagent for 30 minutes. The sections were then treated with 3,3′-diaminobenzidine (DAB) and hydrogen peroxide. A toning solution (DAB Enhancer, Dako) was used to enrich the final color. The sections were counterstained with hematoxylin, dehydrated, and

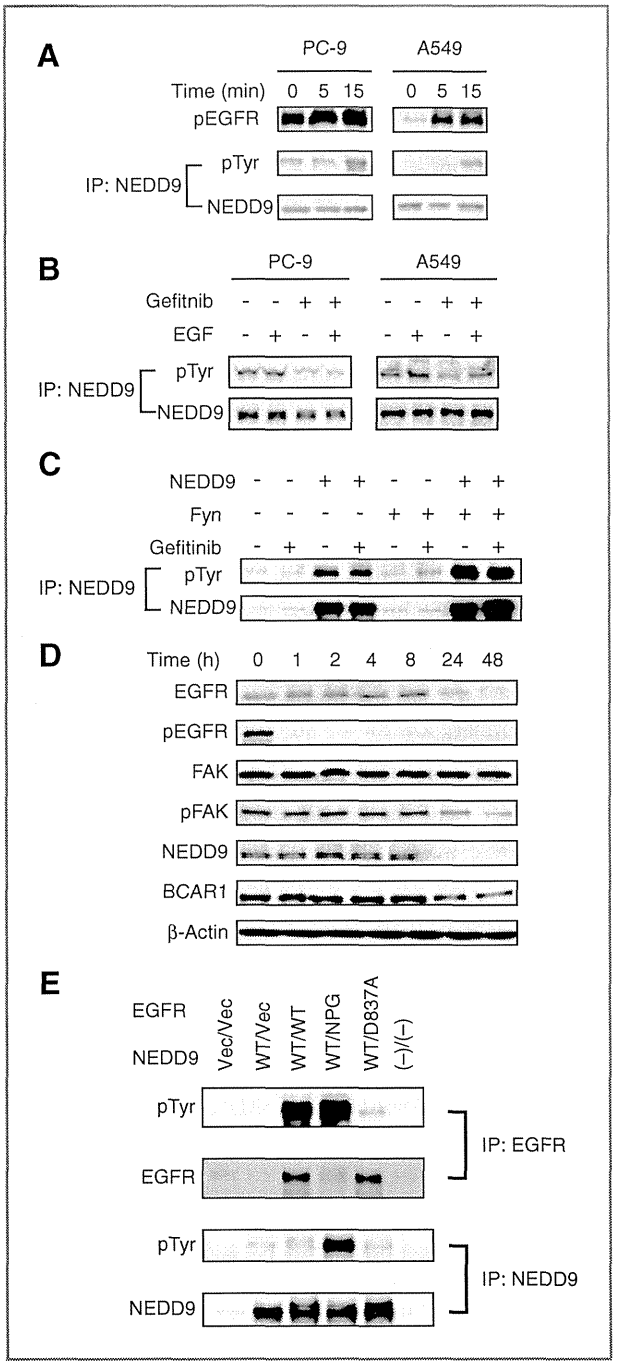

Figure 1. A, EGF stimulation promotes phosphorylation of NEDD9 in human NSCLC cell lines. PC-9 cells and A549 cells were treated with EGF (10 ng/mL) for the indicated time period and then the cells were lysed by scraper in the lysis buffer. Lysates were immunoprecipitated with anti-NEDD9 pAb. The lysates and immunoprecipitates were subjected to immunoblotting with the indicated antibodies. IP, immunoprecipitate; NEDD9, anti-NEDD9 mAb; pEGFR, anti-phospho-EGFR pAb; pTyr, anti-phosphotyrosine mAb. B, inhibition of EGFR by gefitinib downregulates tyrosine phosphorylation of NEDD9 in NSCLC cell lines. PC-9 and A549 cells were cultured in the presence or absence of gefitinib (0.2 μmol/L) for 2 hours and the cells were then treated in the same manner as A. C, gefitinib does not inhibit Fyn-mediated tyrosine phosphorylation of NEDD9 in 293T cells. 293T cells (6×10^6 cells) were transfected with expression plasmid pSRα NEDD9 (NEDD9) and/or pME18S Fyn (Fyn) by FuGENE6. After 48 hours, the cells were lysed and immunoprecipitated with anti-NEDD9 pAb. Treatment with gefitinib (0.2 μmol/L) was conducted during 2 hours before the cell lysis. The immunoprecipitates were subjected to immunoblotting with the indicated antibodies. D, inhibition of EGFR by gefitinib modulates FAK, NEDD9, and BCAR1 in PC-9 cells. PC-9 cells were treated with 0.2 μmol/L gefitinib for the indicated time period. The cells were lysed by scraper in the lysis buffer. The lysates were then subjected to immunoblotting with the indicated antibodies. BCAR1, anti-BCAR1 mAb; β-actin, anti-β-actin mAb; EGFR, anti-EGFR pAb; FAK, anti-FAK mAb; NEDD9, anti-NEDD9 mAb; pFAK, anti-phospho-FAK Ab. E, constitutively active EGFR tyrosine phosphorylates NEDD9 in 293T cells. 293T cells (6×10^6 cells) were co-transfected with pBabe puro EGFR (wild-type or mutants) and pSRα NEDD9 (wild-type) by FuGENE6. At 24 hours after transfection, the cells were detached by trypsin/EDTA and cultured in suspension with serum-starved condition. At 48 hours after transfection, the cells were lysed and immunoprecipitated with anti-NEDD9 pAb or anti-EGFR pAb. The immunoprecipitates were subjected to SDS-PAGE and immunoblotting with the indicated antibodies. Combination of the vectors is as follows: Vec/Vec, pSRα/pBabe puro; WT/Vec, pSRα NEDD9/pBabe puro; WT/WT, pSRα NEDD9/pBabe puro EGFR WT; WT/NPG, pSRα NEDD9/pBabe puro EGFR NPG (constitutively active); WT/D837A, pSRα NEDD9/pBabe puro EGFR D837A (kinase dead); (–)/(–), no plasmids (FuGENE6 alone).

coverslipped. Immunostaining for each sample was determined to be positive (defined as ≥30% positive cells) or negative (<30% positive cells) in a blind fashion by the participating pathologist. We compared 3 cutoff values for NEDD9 positivity (10%, 30%, and 50%) and chose 30%.

Statistical analysis

The χ^2 analysis was applied for the comparison of dichotomous variables. The Kaplan–Meier estimate was used for recurrence-free survival (RFS) and overall survival (OS) analysis, and the log-rank test was used to compare the difference. The Cox proportional hazards model was applied in univariate and multivariate survival analysis to test independent prognostic factors. The control groups of all statistical analyses were usually the first groups in the panels unless specified otherwise in the figure legends. All the statistical analyses were conducted by SPSS Statistics 17 (IBM Corporation) at the 0.05 level of significance.

Clinical investigation was conducted according to Declaration of Helsinki principles. The written informed consent was received from patients before inclusion in this study.

Results

EGF enhances NEDD9 tyrosine phosphorylation

To examine the role of NEDD9 in EGFR signaling pathway in NSCLCs, we first used NSCLC cell lines PC-9 and A549. As shown in Fig. 1A, stimulation with EGF elevated the level of tyrosine phosphorylation of NEDD9 in both PC-9 and A549 cells. Because PC-9 harbors activating mutation of EGFR (ΔE746-A750), the basal level of tyrosine phosphorylation of endogenous EGFR was significantly higher than that of A549 cells with the wild-type EGFR. A TKI for EGFR, gefitinib, abolished the increase in tyrosine phosphorylation of NEDD9 induced by EGF in those cells (Fig.

1B). To assess the specificity of EGFR-mediated tyrosine phosphorylation of NEDD9, we next used the human embryonic kidney cell line 293T cells. As shown in Fig. 1C, gefitinib did not alter the level of tyrosine phosphorylation of NEDD9 caused by exogenous Fyn, an Src family tyrosine kinase in 293T cells. Time course experiments showed that the treatment of PC-9 cells with gefitinib downregulated not only tyrosine phosphorylation of EGFR but also that of FAK. Interestingly, the protein amounts of EGFR, NEDD9, and NEDD9 homologue BCAR1 were also reduced following the addition of gefitinib (Fig. 1D).

In NSCLCs, a variety of activating mutations or deletions have been found in EGFR to correlate with poor clinical outcome. To evaluate the effect of such gene alterations on the tyrosine phosphorylation of NEDD9 *in vitro*, we next conducted co-transfection analysis using 293T cells in suspension culture with serum starvation. As a result, co-transfection of constitutively active mutant EGFR D770-N771 (EGFR NPG) promoted significant level of tyrosine phosphorylation of NEDD9 despite its relatively low level of protein expression, whereas other EGFR constructs including wild-type EGFR and the kinase-negative mutant D837A did not alter the level of tyrosine phosphorylation of NEDD9 (Fig. 1E). However, immunoprecipitation and co-localization analysis revealed that these EGFR constructs and NEDD9 did not co-precipitate and co-localize only marginally (data not shown). These results therefore suggest that the EGFR signaling pathway may modulate tyrosine phosphorylation of NEDD9 in an indirect manner.

Exogenous NEDD9 enhances migratory and invasive potential of NSCLC cell lines

We previously showed that transfected NEDD9 upregulated the motility of Jurkat T cell line on fibronectin (FN) and/or anti-CD3 mAb (23). To determine the association between the expression level of NEDD9 and migratory or invasive behavior of NSCLCs, we used full-length construct for NEDD9, a point mutant NEDD9 F in which the Src SH2-binding motif YDYVHL was mutated to FDFVHL, and a series of deletion mutants: NEDD9 ΔSH3 lacking N-terminal SH3 domain (binding site for FAK and Pyk2); NEDD9 ΔSD lacking the substrate domain (binding site for Crk, Nck), NEDD9 ΔC lacking the C-terminal half, NEDD9 ΔYDYHL lacking from the C-terminus to the YDYVHL motif, NEDD9 ΔCC lacking from the C-terminus to the coiled-coil domain, NEDD9 ΔHLH lacking from the C-terminus to the helix-loop-helix domain (24). The structures of these mutants were schematically summarized in Fig. 2A. In Fig. 2B, we showed the protein expression of these constructs of NEDD9 in the A549 stable transformants.

As shown in Fig. 2C–F, gene transfer of the wild-type NEDD9 into PC-9 and A549 conferred significant enhancement of cell motility (Fig. 2C and D), as well as increasing their invasive potential into Matrigel, which is rich in basement membrane proteins (Fig. 2E and F). This enhancement of EGF- or EGF/integrin-mediated cell migration and invasion was markedly reduced by the addition of gefitinib, suggesting the importance of EGF/EGFR signaling in metastasis and invasion of NSCLCs. Of particular interest is that addition of gefitinib also reduced the fibronectin-mediated cell migration in the absence of exogenous EGF (Figs. 2C and D and 3C and D), suggesting a possible role for NEDD9 in the crosstalk of integrin and EGFR.

We next conducted migration assay of A549 cells with a set of NEDD9 mutants in the presence of EGF (Fig. 2G). As shown in the figure, deletion of SH3, SD domain, or the domains from C-terminus to SD abolished the motility-enhancing effect of NEDD9 completely. On the other hand, mutation or deletion of Src SH2-binding motif reduced this activity in a less efficient manner. The set of experiments involving serial C-terminal deletions suggest that the C-terminal region (CT) may regulate the biologic effect of NEDD9 to a certain degree. These results also show that exogenous expression of NEDD9 promotes cancer cell migration and invasion. In addition, the SH3, SD, and SR domains of NEDD9 are particularly important for EGF/integrin-induced cell motility.

Gene ablation of NEDD9 or BCAR1 reduces the migratory and invasive activity of NSCLC cell lines

To further confirm the enhancing effect of NEDD9 on cell motility and invasiveness of NSCLCs, we conducted gene knockdown studies involving endogenous NEDD9 and its related protein BCAR1 by transfecting PC-9 and A549 with their respective siRNA. Concerning to the off-targeting effect, we evaluated 3 siRNAs (siRNA-1: UCCCAUGCAGGAGACUGCCUCCAGU, siRNA-2: UCCCAGGCAACCGGGUGAAGCUUCU, and siRNA-3: CCUUAUAUGACAAUGUCCCAGAGUG) for NEDD9 in their inhibitory effects and in cDNA rescue experiments and selected siRNA-1 (Supplementary Fig. S1).

As shown in Fig. 3, introduction of NEDD9-specific siRNA abolished not only fibronectin-induced cell migration and invasion but also EGF-induced cell invasion. The BCAR1-specific siRNA also reduced cell migration and invasion, although its inhibitory effect was less than that of NEDD9-specific siRNA in NSCLC cell lines.

Together, results of the gene transfer and gene knockdown experiments suggest that NEDD9 as well as BCAR1 seem to be indispensable factors for EGF as well as integrin-mediated cell motility and invasiveness in NSCLCs.

Gene transfer of NEDD9 into an NSCLC cell line promotes lung metastasis *in vivo*

Our data showing the enhancing effects of NEDD9 on cell motility and invasion of NSCLC cell lines led us to evaluate a xenograft transplantation model using immunodeficient mice (NOG mice) and BLI (34). For this purpose, we used the poorly differentiated human lung adenocarcinoma cell line PC-14 which is negative for NEDD9 at the protein level (Fig. 4A). Figure 4B shows stable expression of transfected NEDD9 (wild-type) in PC-14 cells as long as 28 days after xenotransplantation into NOG mice. The bioluminescence images of xenograft-transplanted NOG mice revealed a positive signal in the lung region of mice transplanted with

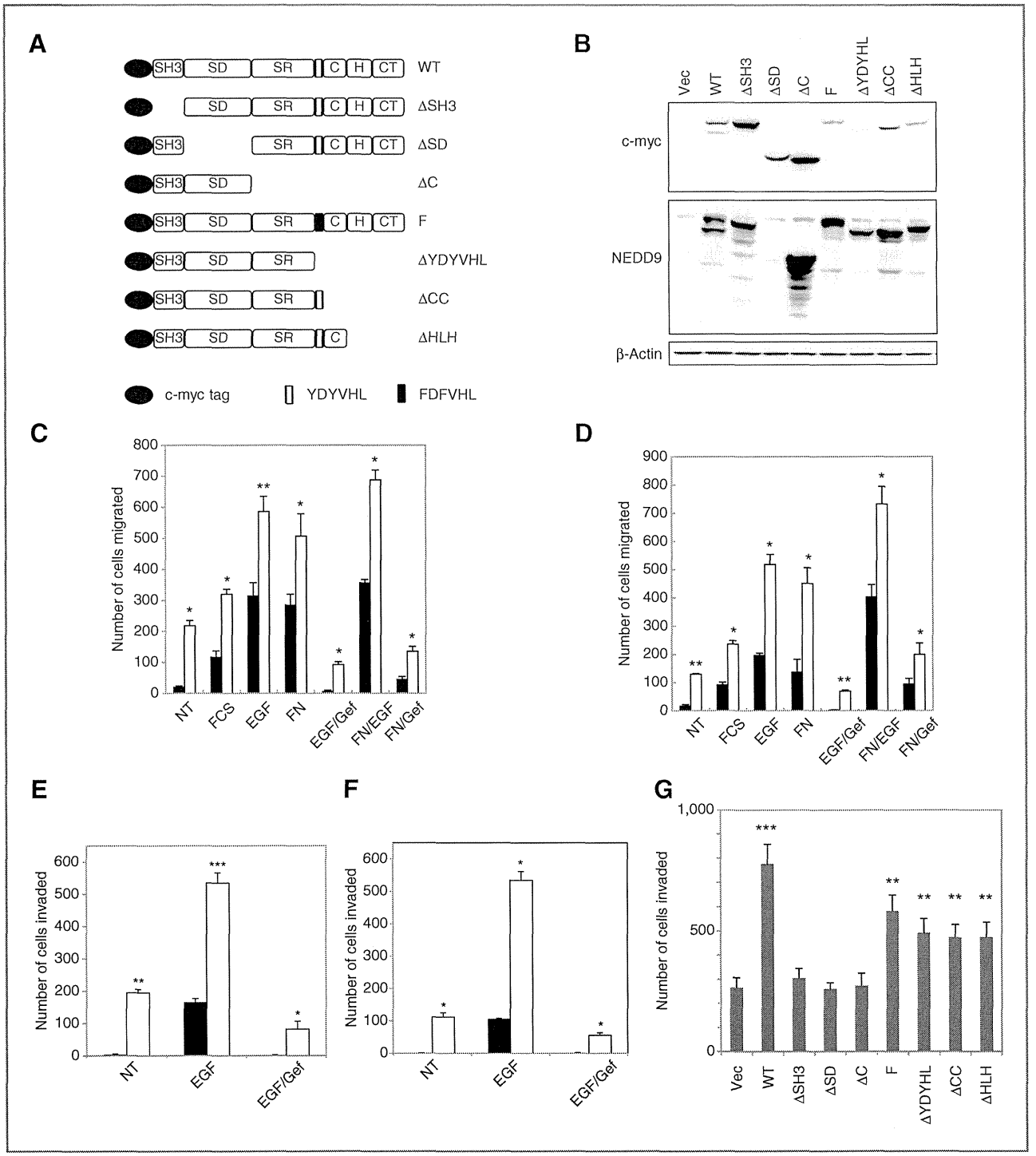

Figure 2. Exogenous NEDD9 enhances migratory and invasive potential of NSCLC cell lines. A, structure of NEDD9 and its mutants. The secondary structure of NEDD9 is graphically shown. From 5′, closed oval, c-myc tag; SH3, Src homology 3 domain; SD, substrate domain; SR, serine-rich region; C, coiled-coil domain; H, helix-loop-helix domain; CT, C-terminal region. B, protein expression of NEDD9 and its mutants in A549 NEDD9 transfectants. A549 cells were transfected with the indicated NEDD9 constructs. After establishing stable transformants, the cell lysates were subjected to immunoblotting with the indicated antibodies (c-myc, anti-c-myc mAb). Vec, BCMG hygro. C–F, transfection of wild-type NEDD9 promotes migratory activity of NSCLC cell lines. PC-9 (C and E) and A549 cells (D and F) were transfected with either empty vector BCMG hyg (closed bar) or BCMG hyg c-myc NEDD9 WT (open bar). The stable transformants were subjected to cell migration assay (C and D) or cell invasion assay (E and F) in the presence or absence of the indicated reagents. NT (nontreated), fetal calf serum (FCS), 10% in the lower chamber; EGF, 10 ng/mL in the lower chamber; FN, inserts were coated with 0.5 μg/mL of fibronectin; Gef, gefitinib in both chambers at 0.2 μmol/L. Statistical significance was evaluated by comparison with NT. *, $P < 0.01$; **, $P < 0.001$; ***, $P < 0.0001$. G, motility-enhancing effect of a series of NEDD9 mutants. A549 NEDD9 transfectants were subjected to the cell migration assay in the presence of EGF (10 ng/mL). Statistical significance was evaluated by comparison with Vec (BCMG hygro).

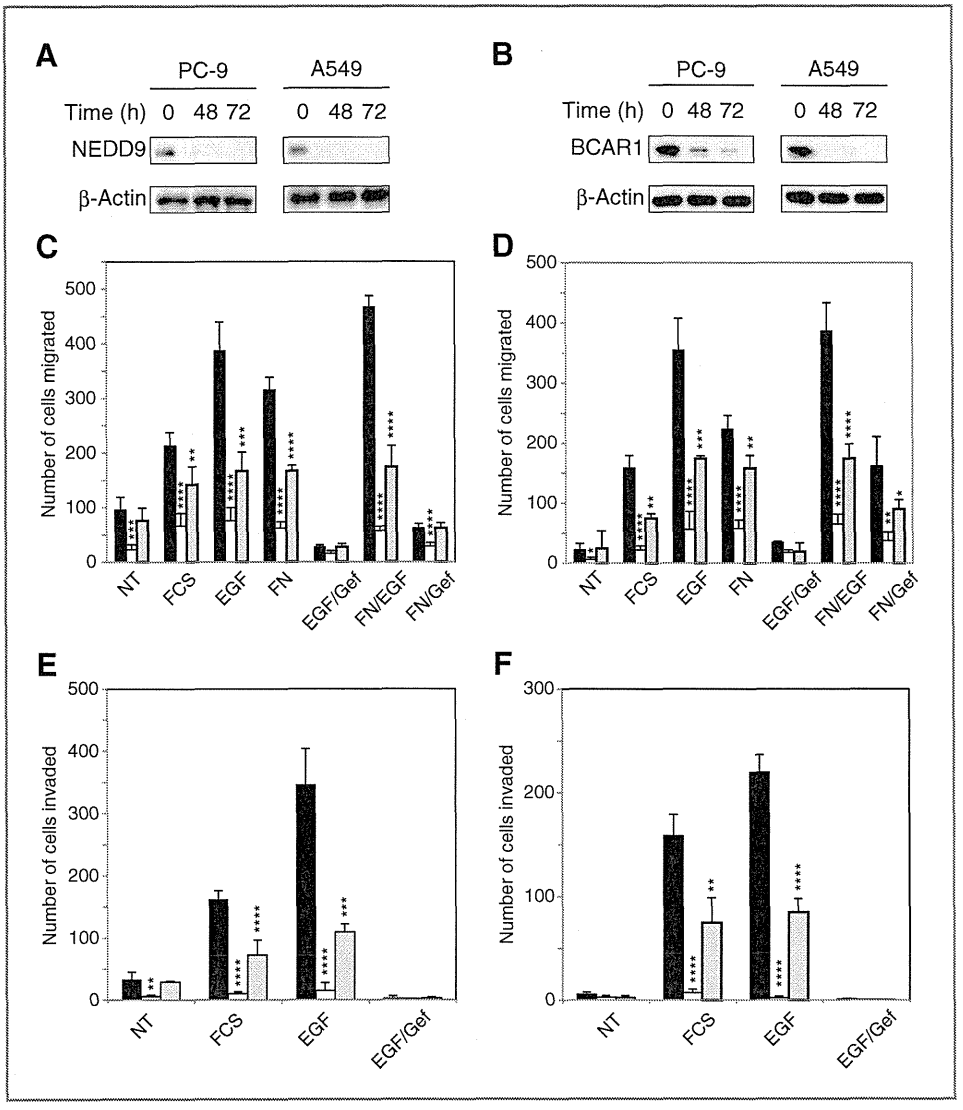

Figure 3. Gene ablation of NEDD9 reduces the migratory and invasive activity of NSCLC cell lines. A and B, protein expression levels of NEDD9 (A) and BCAR1 (B) in PC-9 and A549 cells transfected with their respective specific siRNAs. The cells were lysed 48 or 72 hours following transfection, and equivalent amounts of lysates were subjected to SDS-PAGE and blotted with the indicated antibodies. C–F, transfection of siRNA for NEDD9 or BCAR1 abolishes cell motility and invasiveness of NSCLC cell lines. PC-9 cells (C and E) and A549 cells (D and F) were transfected with siRNA for NEDD9 (open bar), BCAR1 (gray bar), or Stealth RNAi Negative Control (black bar) and subjected to cell migration assay (C and D) and cell invasion assay (E and F) in the presence or absence of the indicated reagents in the lower chamber. NT (nontreated control), fetal calf serum (FCS), 10%; EGF, 10 ng/mL in the lower chamber; FN (fibronectin), coated at 5 μg/mL; Gef (gefitinib), supplemented in both chamber at 0.2 μmol/L. Statistical significance was evaluated by comparison with negative control of each set of three data (Negative control, NEDD9 siRNA, and BCAR1 siRNA). *, $P < 0.05$; **, $P < 0.01$; ***, $P < 0.001$; ****, $P < 0.0001$.

PC-14 co-expressing luciferase and wild-type NEDD9 (Fig. 4C). A region of interest (ROI) of a fixed size was then set in the chest of these mice, and the mean signal intensity (photons/sec/cm^2/steradian) in the ROI was determined. In particular, for the mice transplanted with PC-14 co-expressing luciferase and wild-type NEDD9, the mean signal intensity of the ROI was $5.69 \times 10^3 \pm 0.64$ for the right lung and $10.33 \times 10^3 \pm 2.65$ for the left lung, whereas the mean signal intensity of the ROI was $1.23 \times 10^3 \pm 1.03$ for the right lung and $1.42 \times 10^3 \pm 0.66$ for the left lung of mice transplanted with control PC-14 cells expressing luciferase alone, a greater than 3 times higher signal intensity in the case with the PC-14 NEDD9 transformant. These results suggest that overexpression of NEDD9 promotes *in vivo* lung metastasis of a xenograft-transplanted NSCLC cell line in NOG mice. We next conducted metastasis assays in NOG mice with PC-14 NEDD9 mutants (ΔSH3 and ΔC). We found that subcutaneous injections of these cell lines resulted in detectable tumors in NOG mice. However, the sizes of the primary tumors were less than tumors created by PC-14 vector transfectant and NEDD9 wild-type transfectant. Furthermore, by microscopic examination, we could not detect any metastatic lesions in the lungs of these mice, indicating that these NEDD9 mutants displayed a dominant-negative effect on cell metastasis as well as tumor growth (Fig. 4D and E).

Expression of NEDD9 in human NSCLCs is associated with poor prognosis in lung cancer patients

To determine the clinical relevance of NEDD9 expression in human NSCLCs, we evaluated NEDD9 expression in the primary lesions of human lung adenocarcinoma and also examined the available clinical information of 60 patients treated consecutively at Keio University Hospital with curative surgery between 1999 and 2001. Clinical characteristics of these patients are summarized in Supplementary Tables S1 and S2. By immunohistochemical method, significant expression of NEDD9 protein was identified in 46.7% (28

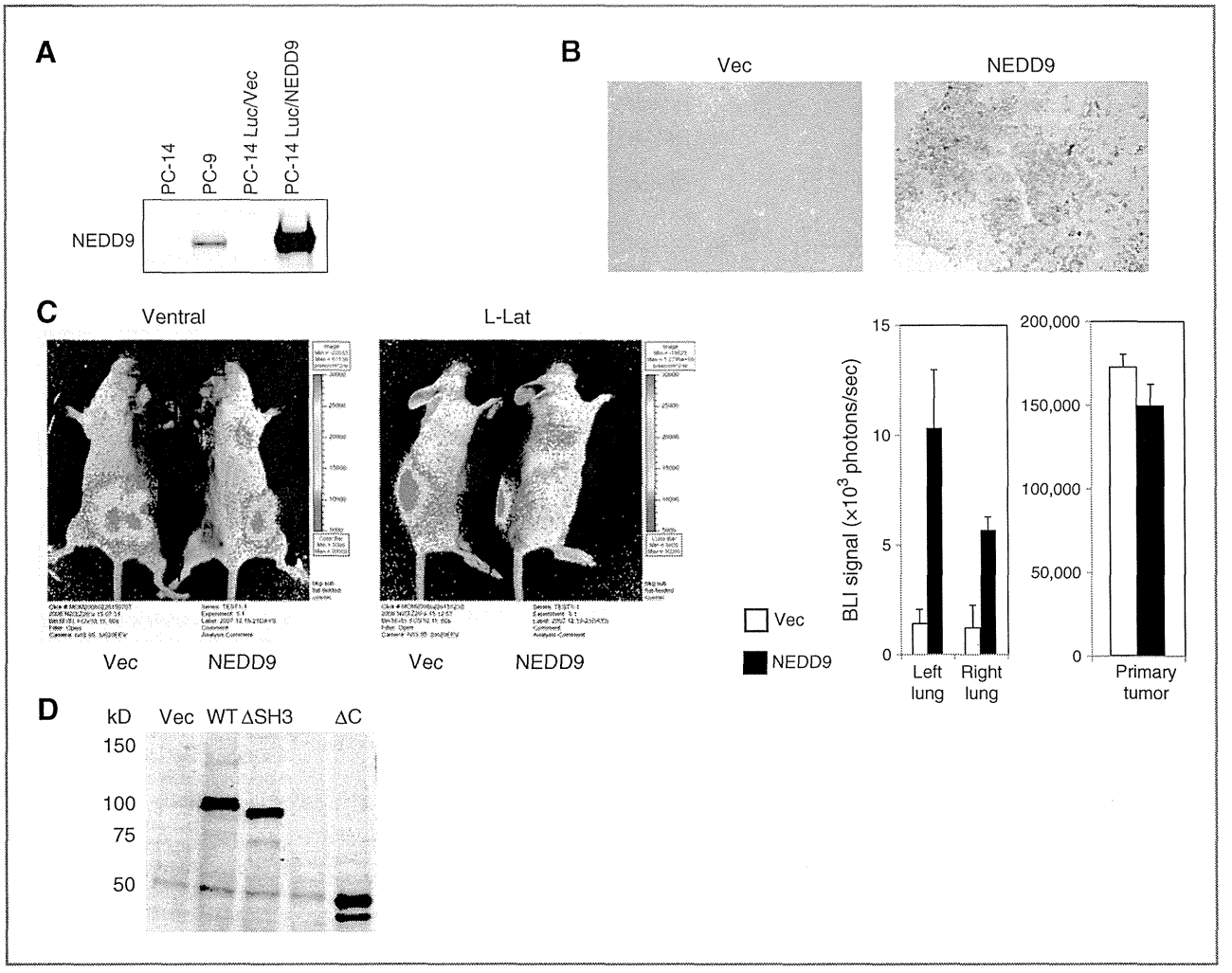

Figure 4. Gene transfer of NEDD9 into the NSCLS cell line PC-14 promotes lung metastasis in NOG mice. A, expression of transfected NEDD9 in PC-14 cells. PC-14 cells were serially transfected with pMX-luc/neo and BCMG hygro c-myc NEDD9 WT (PC-14 Luc/NEDD9) or pMX-luc/neo and BCMG hygro (PC-14 Luc/Vec) by Lipofectamine 2000. Stable clones were established by selection with G418 (1 mg/mL) and hygromycin B (0.2 mg/mL). The equivalent protein extracts from these transformants, parental PC-14 cells, and PC-9 cells were subjected to immunoblotting analysis with anti-NEDD9 mAb. B, immunohistochemical staining for NEDD9 in primary NSCLC tumors. NOG mice underwent subcutaneous transplantation of PC-14 Luc/Vec or PC-14 Luc/NEDD9. At necropsy on day 28 after BLI, the primary tumors were resected, and immunohistochemical method was used to aid in the visualization of NEDD9. C, *in vivo* BLI. NOG mice transplanted of PC-14 Luc/Vec or PC-14 Luc/NEDD9 were subjected to BLI procedure on day 28. Ventral and left-lateral (L-Lat) images were obtained after injection of D-luciferin intraperitoneally. Left, representative BLI. Right, the mean signal intensity of ROI was plotted with error bar ($n = 2$). White bar, PC-14 Luc/Vec; black bar, PC-14 Luc/NEDD9. D, expression of transfected NEDD9 in PC-14 cells. Immunoblotting of PC-14 cells stably transfected with BCMG hygro (Vec), BCMG hygro c-myc NEDD9 WT (WT), BCMG hygro c-myc NEDD9 ΔSH3 (ΔSH3), BCMG hygro c-myc NEDD9 ΔC (ΔC). Blotting was conducted with anti-c-myc mAb (9E10).

of 60) of primary human lung adenocarcinoma tissues (Fig. 5A). Overexpression of NEDD9 was associated with increasing invasion into mediastinal (N2) lymph node ($P = 0.01$), pathologic lymphatic invasion ($P = 0.03$), and pathologic venous invasion ($P = 0.03$; Fig. 5B). However, no other statistically significant correlation was found in lung cancer between NEDD9 expression and other clinical parameters, such as age, sex, smoking history, and the extent of primary tumor (Table 1).

With a median follow-up time of 58.5 months (range, 7–91 months), the median RFS was significantly longer in the NEDD9-negative group (not reached) than in the NEDD9-positive group (23 months; $P < 0.001$; Fig. 5C). The HR for RFS was 4.24 [95% confidence interval (CI), 1.93–9.26] in the NEDD9-positive group. The median OS was also significantly longer in the NEDD9-negative group (not reached) than in the NEDD9-positive group (36 months; $P < 0.001$; Fig. 5C).

In univariate Cox analysis, the HR for OS was 5.35 (95% CI, 1.98–14.50) in the NEDD9-positive group. In addition, N2 invasion and pathologic lymphatic invasion were also significant predictors by univariate analysis. In multivariate Cox analysis, NEDD9 expression (HR, 3.88; 95% CI, 1.34–11.23; $P = 0.01$) and pathologic lymphatic invasion (HR,

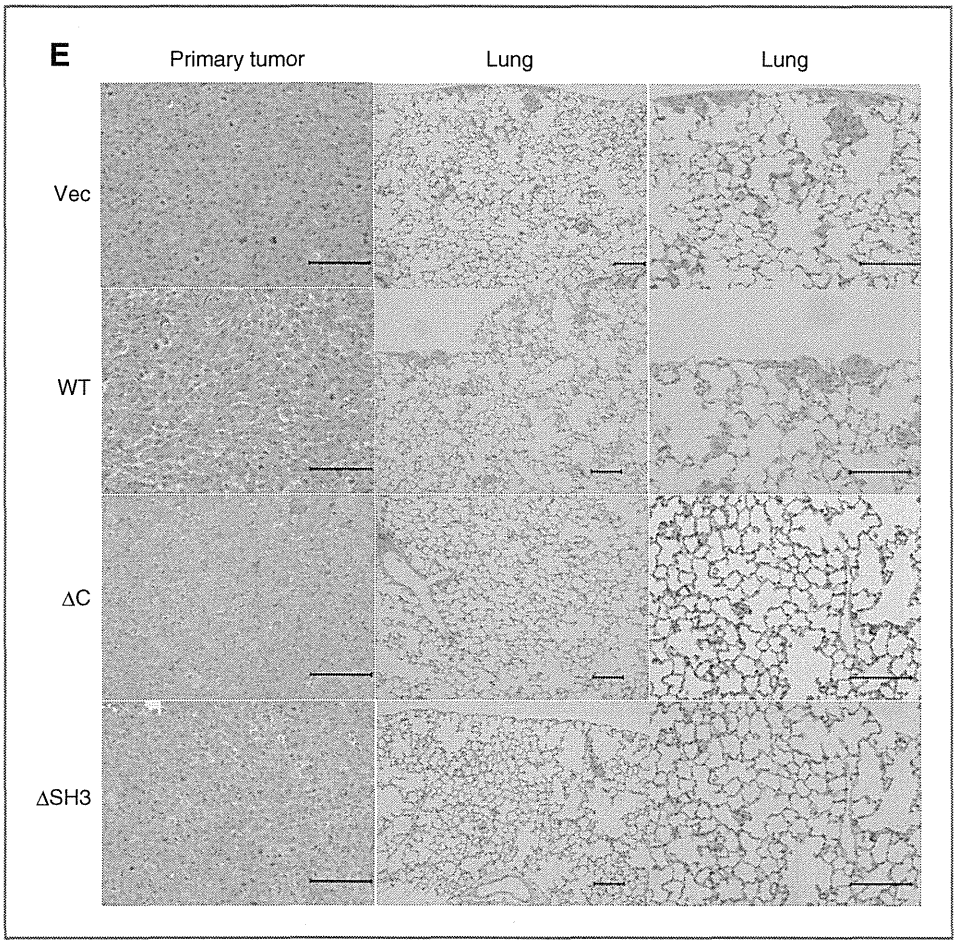

Figure 4. (*Continued*) E, H&E staining of lung tissue from the xenograft-transplanted NOG mice. At necropsy on day 28, the primary tumors and lung tissues were removed from the NOG mice transplanted with each PC-14 transfectant shown in D and stained with H&E. Vec, PC-14 BCMG hygro; WT, PC-14 BCMG hygro c-myc NEDD9 WT; ΔC, PC-14 BCMG hygro c-myc NEDD9 ΔC; and ΔSH3, PC-14 BCMG hygro c-myc NEDD9 ΔSH3. Each scale bar corresponds to 100 μm.

4.94; 95% CI, 1.04–23.5; $P = 0.04$) were independent prognostic variables (summarized in Table 1). Taken together, these results suggest that the expression of NEDD9 closely correlates with venous and lymphatic invasion of cancer cells, and NEDD9 may also be a predictive biomarker for the recurrence and prognosis of human NSCLCs in the clinical setting.

Discussion

In the present study, we showed that tyrosine phosphorylation of NEDD9 was reduced by the inhibition of EGFR in NSCLC cell lines. A constitutively active mutant of EGFR promoted tyrosine phosphorylation of NEDD9 in the absence of integrin signaling. The gene transfer and gene knockdown studies revealed that NEDD9 plays a pivotal role in cell migration and invasion of NSCLC cell line. Overexpression of NEDD9 was shown to promote lung metastasis of an NSCLC cell line in a murine xenograft transplantation model. Finally, the evaluation of the clinical specimens of NSCLCs revealed a strong correlation between NEDD9 expression and RFS or OS, suggesting that NEDD9 is a promising prognostic biomarker in NSCLCs. This is the first study to show the clinical importance of NEDD9 as a prognostic factor as well as the crosstalk between EGFR and NEDD9 signaling pathways in NSCLCs.

Several protein tyrosine kinases (PTK) phosphorylate NEDD9, including FAK (21, 22), RAFTK/Pyk2 (20), Src family PTKs (20, 21), platelet-derived growth factor receptor (PDGFR; ref. 36), Abl (17), and Bcr-Abl (37), many of which are involved in cancer progression and growth. EGFR and PDGFR are RTKs (3) that crosstalk with integrins (8–10, 12), with EGFR physically associating with α5β1 (38) and PDGFR with αvβ3 (39). Engagement of EGFR modulates tyrosine phosphorylation of BCAR1, mediated partly by Src (9), whereas engagement of integrins induces tyrosine phosphorylation of EGFR, mediated by BCAR1 and Src (40, 41). FAK is also a necessary component for EGFR- and PDGFR-induced cell motility (42). These reports suggest that RTKs and integrins form a macromolecular signaling complex at least transiently and have reciprocally compensatory roles in contributing to cell migration and invasion. In this study, we show that NEDD9 may also be an integrator of EGFR and β1-integrin in phosphorylation-dependent signaling, leading to cell migration and invasion of NSCLCs. In this regard, it is possible that other molecules may be associated with EGFR in regulating NEDD9 tyrosine phosphorylation, and additional work is needed to further characterize the signaling complex involving NEDD9, EGFR, and β1-integrins in tumorigenesis and metastasis of NSCLCs.

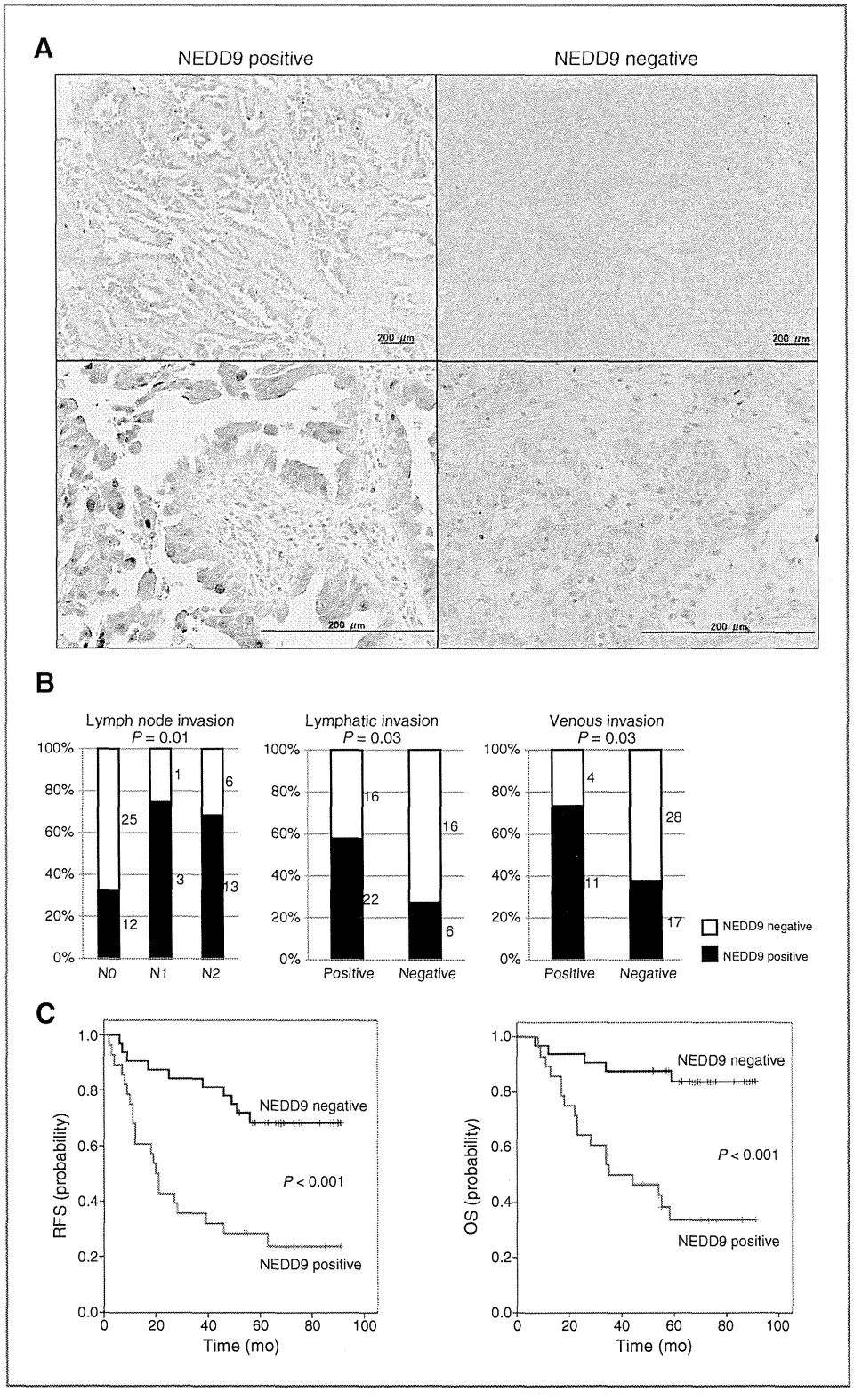

Figure 5. Clinical relevance of NEDD9 expression in NSCLCs. A, immunohistochemical analysis of NEDD9 in primary human lung adenocarcinoma tissues. Top left and bottom left, representative positive staining for NEDD9. Top right and bottom right, representative negative staining for NEDD9. Each scale bar corresponds to 200 μm. B, χ^2 analysis of NEDD9 expression and pathologic invasion of NSCLCs. Left, NEDD9 expression was negative in 68% and positive in 32% in N0, negative in 25% and positive in 75% in N1, negative in 32% and positive in 68% in N2, pathologic node invasion ($P = 0.01$). Middle, NEDD9 expression was negative in 42% and positive in 58% in pathologic lymphatic invasion ($P = 0.03$). Right, NEDD9 expression was negative in 27% and positive in 73% in pathologic venous invasion ($P = 0.03$). C, left, Kaplan–Meier curves for RFS according to NEDD9 expression. Right, Kaplan–Meier curves for OS according to NEDD9 expression.

PC-9 cells used in this study harbors an in-frame deletion in EGFR which causes the receptor to be constitutively activated as a result of structural change proximal to the ATP-binding site (43). These cells and a significant population of NSCLC tumor cells are dependent on the constitutively activated EGFR, thus blockade of the signal by gefitinib results in apoptotic cell death (6, 7). In the context of oncogene involvement in tumor growth, of particular

Table 1. Cox univariate and multivariate analysis of patients with NSCLCs

	RFS		OS	
	HR (95% CI)	***P***	**HR (95% CI)**	***P***
Univariate analysis				
NEDD9 (positive vs. negative)	4.24 (1.93–9.26)	<0.001	5.35 (1.98–14.50)	0.001
Sex (male vs. female)	1.08 (0.53–2.20)	0.83	1.3 (0.56–3.00)	0.54
Age (>65 y)	1.17 (0.58–2.38)	0.66	1.11 (0.49–2.51)	0.8
Smoking history (smoker vs. non-smoker)	1.19 (0.58–2.39)	0.65	1.25 (0.55–2.84)	0.59
pStage (III vs. I–II)	2.42 (1.20–4.91)	0.01	3.1 (1.35–7.13)	0.01
N1 (positive vs. negative)	1.45 (0.35–6.12)	0.61	1.22 (0.16–9.09)	0.85
N2 (positive vs. negative)	3.9 (1.91–7.97)	<0.001	4.8 (2.05–11.21)	<0.001
Lymphatic invasion (positive vs. negative)	5.83 (2.23–15.28)	<0.001	10.1 (2.36–43.2)	0.002
Venous invasion (positive vs. negative)	1.85 (0.85–4.06)	0.12	2.713 (1.17–6.29)	0.02
Multivariate analysis				
NEDD9 (positive vs. negative)	3.08 (1.37–6.93)	0.006	3.88 (1.34–11.23)	0.01
pStage (III vs. I–II)	0.78 (0.24–2.5)	0.67	1.32 (0.38–4.47)	0.66
N2 (positive vs. negative)	2.54 (0.76–8.46)	0.13	1.84 (0.53–6.39)	0.34
Lymphatic invasion (positive vs. negative)	4.84 (1.52–15.37)	0.008	4.94 (1.04–23.5)	0.04
Venous invasion (positive vs. negative)	0.62 (0.26–1.44)	0.26	0.79 (0.31–1.99)	0.62

interest is that blockade of EGFR signal caused not only dephosphorylation but also a reduction in the protein levels of focal adhesion resident proteins such as BCAR1 and FAK as well as NEDD9. Because these proteins have been reported to incur caspase-induced degradation in apoptosis (44), the results observed in this study may reflect a gefitinib-induced apoptotic process. Supporting this notion, gene transfer of NEDD9 into PC-9 and A549 cells conferred resistance to the chemotherapeutic reagents such as gefitinib, paclitaxel, and cisplatin (Supplementary Figs. S2 and S3). Future in-depth studies will be conducted to expand on these interesting data.

We and others previously reported that NEDD9 phosphorylation contributes to cell migration and invasion (22, 23, 36, 45). We now show the involvement of NEDD9 in EGFR-mediated cell migration and invasion of NSCLCs. Consistent with previous reports, our studies indicated that BCAR1 siRNA also caused significant reduction in EGFR-mediated cell motility of NSCLCs. Another member of Cas family, BCAR1/p130Cas, was independently identified as the primary gene that confers breast cancer cells with resistance to anti-estrogen (46). HER2/neu is a member of the EGFR family and is a notable therapeutic target of breast cancer, similar to EGFR in NSCLCs (47). Interestingly, a double-transgenic mice of MMTV-BCAR1 and MMTV-HER2/neu developed multifocal mammary tumors with a significant shorter latency than the MMTV-HER2/neu transgenic mice (48). Because elevated expression of HER2 accounts for 3% of NSCLC cases, the interaction between HER2 and NEDD9 and the clinical relevance of BCAR1 in NSCLCs remain to be elucidated as a future goal.

Deletion of SH3 domain or SD domain equivalently affected the EGF/integrin-mediated cell motility and invasiveness. Because FAK associates with SH3 domain and Nck or Crk with SD domain of NEDD9 (14, 17), these kinase and adaptor proteins may be critical components of EGF/integrin-induced NEDD9 functions in NSCLCs. Crk forms complex with DOCK180, Nck with WASP and PAK, with both of these complexes relaying signals to the Rho family GTPases Rac and Cdc42, thereby reorganizing actin cytoskeleton (18). On the basis of the results with YDYVHL mutants, upstream Src family PTKs may also contribute to EGF/integrin-mediated NEDD9 function, in accordance with the recently published reports (9, 40, 41). In view of the result with NEDD9 ΔC, serine-rich region is also important for cellular migration elicited by NEDD9. Of interest is that corresponding region of BCAR1 is recently reported to fold as a 4-helix bundle, a protein interaction motif seen in FAK, α-catenin, and vinculin (49).

In the clinical setting, recent studies have indicated that the expression levels of NEDD9 mRNA and protein were elevated in a variety of malignancies such as melanoma (26), glioblastoma (36), breast cancer (27), and that NEDD9 protein is an essential switch for prometastatic behavior of tumor cells. Indeed, some of these studies described NEDD9 as one of the metastatic signature (25, 27). NEDD9 may function in metastasis of colorectal cancer and head and neck squamous cell carcinoma, processes which potentially involve novel upstream molecules such as hypoxia-inducible factor (28), N-terminal truncated carboxypeptidase E splice isoform (29), Wnt (31), and VEGF (50). Our analysis of the clinical records of patients undergoing surgical resection with curative intent of their NSCLCs (with a recurrence rate within 2 years of specimen collection of 43% being similar to the rate reported previously) to evaluate the potential clinical significance of NEDD9 expression in NSCLCs showed a significant correlation between NEDD9 expression and previously

identified pathologic prognostic factors. Expression of NEDD9 was associated with a significant increase in the risk of metastasis and recurrence, with a corresponding decrease in survival and worsened clinical outcome. Multivariate analysis also suggested that NEDD9 expression is an independent predictive factor for the recurrence of NSCLCs. To evaluate the NEDD9 expression in NSCLCs, we set 3 cutoff values (10%, 30%, 50%). Kaplan–Meier curves in the cases with 10% cutoff and 50% cutoff value are shown in Supplementary Fig. S4. When the cutoff value (% positive cells) was 10%, there was no statistically significant difference in OS and RFS. When the cutoff was 50%, the number of positive cases was only 6. When the cutoff was 30%, significant difference was observed in OS and RFS. It should be noted that these data were derived from a retrospective analysis and are likely to suffer from selection bias. Randomized control study or stratified analysis will be necessary in a future study to extend our present findings.

In conclusion, our present work suggests that NEDD9 is a predictive factor for recurrence and prognosis in NSCLCs. Although a variety of gene profiles have been reported to correlate with recurrence of NSCLCs, none has yet been definitely established (51). Because the clinical records evaluated in this study did not contain genetical information on EGFR mutation, KRAS mutation which may affect the sensitivity to gefitinib (52), further comprehensive analysis is necessary in the next step. Optimal strategies to prevent recurrence and metastasis of NSCLCs may need to incorporate NEDD9 expression as one of the promising predictive factors and NEDD9 itself may be a novel therapeutic target for future NSCLC treatment.

Disclosure of Potential Conflicts of Interest

No potential conflicts of interest were disclosed.

Authors' Contributions

Conception and design: S. Kondo, S. Iwata, H. Kawasaki, H. Tanaka, C. Morimoto

Development of methodology: S. Kondo, S. Iwata, T. Yamada, H. Kawasaki

Acquisition of data (provided animals, acquired and managed patients, provided facilities, etc.): S. Kondo, T. Yamada, Y. Inoue, H. Ichihara, Y. Kichikawa, T. Katayose, A. Souta-Kuribara, Y. Hayashi, K. Kamiya

Analysis and interpretation of data (e.g., statistical analysis, biostatistics, computational analysis): S. Kondo, S. Iwata, T. Yamada, Y. Inoue, Y. Kichikawa, H. Yamazaki, H. Kawasaki, N.H. Dang

Writing, review, and/or revision of the manuscript: S. Kondo, S. Iwata, Y. Kichikawa, O. Hosono, H. Kawasaki, N.H. Dang, C. Morimoto

Administrative, technical, or material support (i.e., reporting or organizing data, constructing databases): S. Kondo, T. Yamada, Y. Inoue, H. Ichihara, A. Souta-Kuribara, H. Yamazaki, O. Hosono, M. Sakamoto

Study supervision: S. Iwata, H. Yamazaki, O. Hosono, H. Kawasaki, H. Tanaka, C. Morimoto

Acknowledgments

The authors thank Jun Suzuki and Yukiko Nagafuji for secretarial assistance.

Grant Support

This work was supported by grants-in aid from the Ministry of Education, Science, Sports and Culture (S. Iwata and C. Morimoto), and Ministry of Health, Labor and Welfare, Japan, and by the Program for Promotion of Fundamental Studies in Health Sciences of the National Institute of Biomedical Innovation (C. Morimoto).

The costs of publication of this article were defrayed in part by the payment of page charges. This article must therefore be hereby marked *advertisement* in accordance with 18 U.S.C. Section 1734 solely to indicate this fact.

Received August 23, 2011; revised August 20, 2012; accepted August 28, 2012; published OnlineFirst October 4, 2012.

References

1. Boyle P, Levin B. International Agency for Research on Cancer, World Health Organization. World cancer report 2008. Lyon, France; Geneva, Switzerland: International Agency for Research on Cancer; Distributed by WHO Press; 2008.
2. Winton T, Livingston R, Johnson D, Rigas J, Johnston M, Butts C, et al. Vinorelbine plus cisplatin vs. observation in resected non-small-cell lung cancer. N Engl J Med 2005;352:2589–97.
3. Schlessinger J. Cell signaling by receptor tyrosine kinases. Cell 2000;103:211–25.
4. Arteaga CL. The epidermal growth factor receptor: from mutant oncogene in nonhuman cancers to therapeutic target in human neoplasia. J Clin Oncol 2001;19:32S–40S.
5. Herbst RS, Khuri FR, Fossella FV, Glisson BS, Kies MS, Pisters KM, et al. ZD1839 (Iressa) in non-small-cell lung cancer. Clin Lung Cancer 2001;3:27–32.
6. Lynch TJ, Bell DW, Sordella R, Gurubhagavatula S, Okimoto RA, Brannigan BW, et al. Activating mutations in the epidermal growth factor receptor underlying responsiveness of non-small-cell lung cancer to gefitinib. N Engl J Med 2004;350:2129–39.
7. Paez JG, Janne PA, Lee JC, Tracy S, Greulich H, Gabriel S, et al. EGFR mutations in lung cancer: correlation with clinical response to gefitinib therapy. Science 2004;304:1497–500.
8. Morello V, Cabodi S, Sigismund S, Camacho-Leal MP, Repetto D, Volante M, et al. β1 integrin controls EGFR signaling and tumorigenic properties of lung cancer cells. Oncogene 2011;30:4087–96.
9. Ricono JM, Huang M, Barnes LA, Lau SK, Weis SM, Schlaepfer DD, et al. Specific cross-talk between epidermal growth factor receptor and integrin alphavbeta5 promotes carcinoma cell invasion and metastasis. Cancer Res 2009;69:1383–91.
10. Walker JL, Assoian RK. Integrin-dependent signal transduction regulating cyclin D1 expression and G1 phase cell cycle progression. Cancer Metastasis Rev 2005;24:383–93.
11. Desgrosellier JS, Cheresh DA. Integrins in cancer: biological implications and therapeutic opportunities. Nat Rev Cancer 2010;10:9–22.
12. ffrench-Constant C, Colognato H. Integrins: versatile integrators of extracellular signals. Trends Cell Biol 2004;14:678–86.
13. Nojima Y, Rothstein DM, Sugita K, Schlossman SF, Morimoto C. Ligation of VLA-4 on T cells stimulates tyrosine phosphorylation of a 105-kD protein. J Exp Med 1992;175:1045–53.
14. Minegishi M, Tachibana K, Sato T, Iwata S, Nojima Y, Morimoto C. Structure and function of Cas-L, a 105-kD Crk-associated substrate-related protein that is involved in beta 1 integrin-mediated signaling in lymphocytes. J Exp Med 1996;184:1365–75.
15. Sakai R, Iwamatsu A, Hirano N, Ogawa S, Tanaka T, Mano H, et al. A novel signaling molecule, p130, forms stable complexes *in vivo* with v-Crk and v-Src in a tyrosine phosphorylation-dependent manner. EMBO J 1994;13:3748–56.
16. Kumar S, Tomooka Y, Noda M. Identification of a set of genes with developmentally down-regulated expression in the mouse brain. Biochem Biophys Res Commun 1992;185:1155–61.
17. Law SF, Estojak J, Wang B, Mysliwiec T, Kruh G, Golemis EA. Human enhancer of filamentation 1, a novel p130cas-like docking protein, associates with focal adhesion kinase and induces pseudohyphal growth in *Saccharomyces cerevisiae*. Mol Cell Biol 1996;16:3327–37.

18. O'Neill GM, Seo S, Serebriiskii IG, Lessin SR, Golemis EA. A new central scaffold for metastasis: parsing HEF1/Cas-L/NEDD9. Cancer Res 2007;67:8975–9.
19. Ohashi Y, Tachibana K, Kamiguchi K, Fujita H, Morimoto C. T cell receptor-mediated tyrosine phosphorylation of Cas-L, a 105-kDa Crk-associated substrate-related protein, and its association of Crk and C3G. J Biol Chem 1998;273:6446–51.
20. Manie SN, Beck AR, Astier A, Law SF, Canty T, Hirai H, et al. Involvement of p130(Cas) and p105(HEF1), a novel Cas-like docking protein, in a cytoskeleton-dependent signaling pathway initiated by ligation of integrin or antigen receptor on human B cells. J Biol Chem 1997; 272:4230–6.
21. Tachibana K, Urano T, Fujita H, Ohashi Y, Kamiguchi K, Iwata S, et al. Tyrosine phosphorylation of Crk-associated substrates by focal adhesion kinase. A putative mechanism for the integrin-mediated tyrosine phosphorylation of Crk-associated substrates. J Biol Chem 1997; 272:29083–90.
22. van Seventer GA, Salmen HJ, Law SF, O'Neill GM, Mullen MM, Franz AM, et al. Focal adhesion kinase regulates beta1 integrin-dependent T cell migration through an HEF1 effector pathway. Eur J Immunol 2001;31:1417–27.
23. Ohashi Y, Iwata S, Kamiguchi K, Morimoto C. Tyrosine phosphorylation of Crk-associated substrate lymphocyte-type is a critical element in TCR- and beta 1 integrin-induced T lymphocyte migration. J Immunol 1999;163:3727–34.
24. Iwata S, Souta-Kuribara A, Yamakawa A, Sasaki T, Shimizu T, Hosono O, et al. HTLV-I Tax induces and associates with Crk-associated substrate lymphocyte type (Cas-L). Oncogene 2005;24:1262–71.
25. Ji H, Ramsey MR, Hayes DN, Fan C, McNamara K, Kozlowski P, et al. LKB1 modulates lung cancer differentiation and metastasis. Nature 2007;448:807–10.
26. Kim M, Gans JD, Nogueira C, Wang A, Paik JH, Feng B, et al. Comparative oncogenomics identifies NEDD9 as a melanoma metastasis gene. Cell 2006;125:1269–81.
27. Minn AJ, Gupta GP, Siegel PM, Bos PD, Shu W, Giri DD, et al. Genes that mediate breast cancer metastasis to lung. Nature 2005;436: 518–24.
28. Kim SH, Xia D, Kim SW, Holla V, Menter DG, Dubois RN. Human enhancer of filamentation 1 Is a mediator of hypoxia-inducible factor-1alpha-mediated migration in colorectal carcinoma cells. Cancer Res 2010;70:4054–63.
29. Lee TK, Murthy SR, Cawley NX, Dhanvantari S, Hewitt SM, Lou H, et al. An N-terminal truncated carboxypeptidase E splice isoform induces tumor growth and is a biomarker for predicting future metastasis in human cancers. J Clin Invest 2011;121:880–92.
30. Li Y, Bavarva JH, Wang Z, Guo J, Qian C, Thibodeau SN, et al. HEF1, a novel target of Wnt signaling, promotes colonic cell migration and cancer progression. Oncogene 2011;30:2633–43.
31. Xia D, Holla VR, Wang D, Menter DG, DuBois RN. HEF1 is a crucial mediator of the proliferative effects of prostaglandin E(2) on colon cancer cells. Cancer Research 2010;70:824–31.
32. Koizumi F, Shimoyama T, Taguchi F, Saijo N, Nishio K. Establishment of a human non-small cell lung cancer cell line resistant to gefitinib. Int J Cancer 2005;116:36–44.
33. Greulich H, Chen TH, Feng W, Janne PA, Alvarez JV, Zappaterra M, et al. Oncogenic transformation by inhibitor-sensitive and -resistant EGFR mutants. PLoS Med 2005;2:e313.
34. Inoue Y, Tojo A, Sekine R, Soda Y, Kobayashi S, Nomura A, et al. *In vitro* validation of bioluminescent monitoring of disease progression and therapeutic response in leukaemia model animals. Eur J Nucl Med Mol Imaging 2006;33:557–65.
35. Ito M, Hiramatsu H, Kobayashi K, Suzue K, Kawahata M, Hioki K, et al. NOD/SCID/gamma(c)(null) mouse: an excellent recipient mouse model for engraftment of human cells. Blood 2002; 100:3175–82.
36. Natarajan M, Stewart JE, Golemis EA, Pugacheva EN, Alexandropoulos K, Cox BD, et al. HEF1 is a necessary and specific downstream effector of FAK that promotes the migration of glioblastoma cells. Oncogene 2006;25:1721–32.
37. de Jong R, van Wijk A, Haataja L, Heisterkamp N, Groffen J. BCR/ABL-induced leukemogenesis causes phosphorylation of Hef1 and its association with Crkl. J Biol Chem 1997;272:32649–55.
38. Lee JW, Juliano RL. The alpha5beta1 integrin selectively enhances epidermal growth factor signaling to the phosphatidylinositol-3-kinase/Akt pathway in intestinal epithelial cells. Biochim Biophys Acta 2002;1542:23–31.
39. Ding Q, Stewart J Jr, Olman MA, Klobe MR, Gladson CL. The pattern of enhancement of Src kinase activity on platelet-derived growth factor stimulation of glioblastoma cells is affected by the integrin engaged. J Biol Chem 2003;278:39882–91.
40. Moro L, Dolce L, Cabodi S, Bergatto E, Boeri Erba E, Smeriglio M, et al. Integrin-induced epidermal growth factor (EGF) receptor activation requires c-Src and p130Cas and leads to phosphorylation of specific EGF receptor tyrosines. J Biol Chem 2002;277: 9405–14.
41. Leung EL, Tam IY, Tin VP, Chua DT, Sihoe AD, Cheng LC, et al. SRC promotes survival and invasion of lung cancers with epidermal growth factor receptor abnormalities and is a potential candidate for molecular-targeted therapy. Mol Cancer Res 2009;7: 923–32.
42. Sieg DJ, Hauck CR, Ilic D, Klingbeil CK, Schaefer E, Damsky CH, et al. FAK integrates growth-factor and integrin signals to promote cell migration. Nat Cell Biol 2000;2:249–56.
43. Sakai K, Arao T, Shimoyama T, Murofushi K, Sekijima M, Kaji N, et al. Dimerization and the signal transduction pathway of a small in-frame deletion in the epidermal growth factor receptor. FASEB J 2006; 20:311–3.
44. Law SF, O'Neill GM, Fashena SJ, Einarson MB, Golemis EA. The docking protein HEF1 is an apoptotic mediator at focal adhesion sites. Mol Cell Biol 2000;20:5184–95.
45. Seo S, Asai T, Saito T, Suzuki T, Morishita Y, Nakamoto T, et al. Crk-associated substrate lymphocyte type is required for lymphocyte trafficking and marginal zone B cell maintenance. J Immunol 2005;175:3492–501.
46. Brinkman A, van der Flier S, Kok EM, Dorssers LC. BCAR1, a human homologue of the adapter protein p130Cas, and antiestrogen resistance in breast cancer cells. J Natl Cancer Inst 2000;92:112–20.
47. Zhou BP, Hung MC. Dysregulation of cellular signaling by HER2/neu in breast cancer. Semin Oncol 2003;30:38–48.
48. Cabodi S, Tinnirello A, Di Stefano P, Bisaro B, Ambrosino E, Castellano I, et al. p130Cas as a new regulator of mammary epithelial cell proliferation, survival, and HER2-neu oncogene-dependent breast tumorigenesis. Cancer Res 2006;66:4672–80.
49. Briknarova K, Nasertorabi F, Havert ML, Eggleston E, Hoyt DW, Li C, et al. The serine-rich domain from Crk-associated substrate (p130cas) is a four-helix bundle. J Biol Chem 2005;280:21908–14.
50. Lucas JT Jr, Salimath BP, Slomiany MG, Rosenzweig SA. Regulation of invasive behavior by vascular endothelial growth factor is HEF1-dependent. Oncogene 2010;29:4449–59.
51. Potti A, Mukherjee S, Petersen R, Dressman HK, Bild A, Koontz J, et al. A genomic strategy to refine prognosis in early-stage non-small-cell lung cancer. N Engl J Med 2006;355:570–80.
52. Hirsch FR, Varella-Garcia M, Bunn PA Jr, Franklin WA, Dziadziuszko R, Thatcher N, et al. Molecular predictors of outcome with gefitinib in a phase III placebo-controlled study in advanced non-small-cell lung cancer. J Clin Oncol 2006;24:5034–42.

改訂版

アスベスト関連疾患早期発見・診断の手引

―中皮腫を正しく診断するために―

独立行政法人　労働者健康福祉機構　監修

岡山労災病院　副院長
アスベスト関連疾患研究センター長 **岸本卓巳**　編

日本医師会推薦

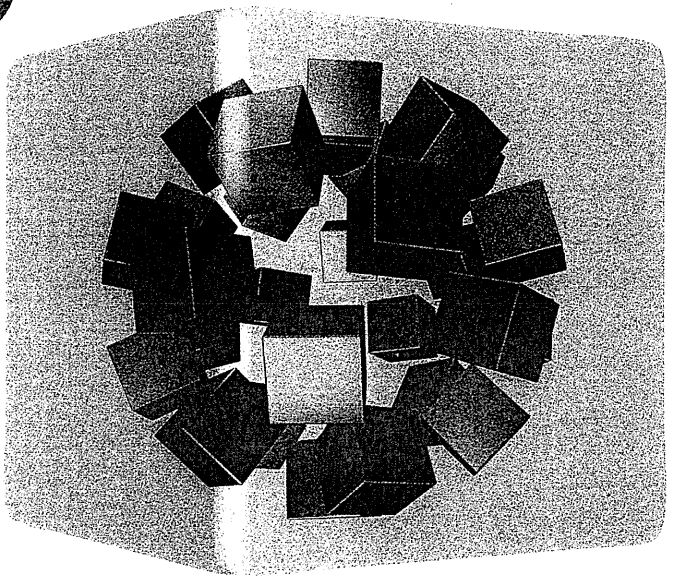

確実な組織診断・鑑別診断を!!

最新症例より、問診や検査所見から診断のポイント、
治療経過までを胸部X線やCT画像とともに立体的に解説―
アスベスト関連疾患の基礎知識、関係法令、諸手続きの解説も充実!!

一般社団法人 日本労務研究会

症例3

一部に骨形成を伴った胸膜中皮腫症例

データBOX

○年齢・性別：60歳代　男性
○受診経緯：近医より専門医療機関を紹介された。
○主　　訴：咳嗽
○既 往 歴：特記すべきことなし
○職 業 歴：元溶接業、現在は木工業に従事していた。
○喫 煙 歴：20歳代前半から40年間、20本／日。
○現 病 歴：専門医療機関受診の1ヶ月前、咳嗽あり近医にて胸部X線で右胸水の貯留を指摘されたため、紹介され精査目的に入院となった。胸部理学所見では右側呼吸音の軽度減弱を認めたが、他に異常所見を認めなかった。表在リンパ節は触知しなかった。

画像あるいは病理診断のポイント

本症例は、骨および軟骨形成を伴う悪性胸膜中皮腫肉腫型の例です。診断時の骨形成はわずかで石灰化胸膜プラークのある胸膜から発生した胸膜中皮腫のような印象を与えます。しかし、対側の左胸膜には石灰化も胸膜プラークも認められません。病理所見では中皮腫肉腫型細胞から骨および軟骨形成する細胞へと連続的に認められ中皮腫による骨形成であることがわかります。化学療法を行いましたが効果なく腫瘍は急速に増大していきました。腫瘍の増大に伴い骨形成も増強していることが胸部CTの変化として確認することができます。本症例は免疫組織染色で骨形成細胞が中皮腫であることが確認できますが、免疫組織染色の結果によっては骨外性骨肉腫との鑑別が困難な場合もあります。

●検査と治療

○血液生化学（表6）、胸部X線（図16）、及び胸部CT所見（図17）

右側胸水の貯留を認めました。胸部X線では指摘困難ですが、胸部CTでは胸膜の不整な肥厚が認められ内部に石灰化を伴っています。血液検査所見では、白血球数9,750/μℓ、CRP 058mg/dℓで著変は認められません。血清中の各種腫瘍マーカー（CEA、CYFRA、SCC、ProGRP）に異常値を認めませんでした。

○入院後経過

右側胸腔穿刺にて淡黄色、清の胸水を採取しました。胸水中の検査値はTP 4.8g/dl, Alb 3.0g/dl, LDH 415IU/L, Glu 92mg/dl, CEA 3.5ng/ml, CYFRA 18ng/ml, ADA 24.1U/L, ヒアルロン酸 83,380ng/mlでした。胸水細胞診では、リンパ球を背景にクロマチンの増量した異型の目立つ大型の異型細胞がみられました。診断確定のために胸腔鏡下胸膜生検を施行しました。胸腔鏡所見では、壁側及び臓側胸膜に播種状に分布した多数の小結節性病変を認めました。その生検標本の病理組織学的検査で胸膜中皮腫、肉腫型と診断しました（**図18**）。一部で腫瘍細胞の軟骨や骨への分化が認められました（**図19**、**表20**）。

○手術所見及び術後経過

入院後、シスプラチン／ペメトレキセドによる化学療法を施行しましたが、胸膜肥厚は増強、肥厚した胸膜内の石灰化も増加しました。ゲムシタビン／ビノレルビンに変更して化学療法を継続しましたが無効でさらに胸膜肥厚は増強、次第に呼吸状態は悪化していき、診断から5ヶ月後に死亡されました。

（青江啓介）